INTERNATIONAL CENTER FOR NUMERICAL METHODS IN ENGINEERING

Pressure Stability in Fractional Step Finite Element Methods for Incompressible Flows

R. Codina

Publication CIMNE Nº-186, March 2000

Pressure stability in fractional step finite element methods for incompressible flows

Ramon Codina

Universitat Politècnica de Catalunya,
Jordi Girona 1-3, Edifici C1, 08034 Barcelona, Spain.
Email: ramon.codina@upc.es, Website: http://www.rmee.upc.es/homes/codina

Abstract

The objective of this paper is to analyze the pressure stability of fractional step finite element methods for incompressible flows. For the classical first order projection method, it is shown that there is a pressure control which depends on the time step size, and therefore there is a lower bound for this time step for stability reasons. The situation is much worse for a second order scheme in which part of the pressure gradient is kept in the momentum equation. The pressure stability in this case is extremely weak. To overcome these shortcomings, a stabilized fractional step finite element method is also considered, and its stability is analyzed. Some simple numerical examples are presented to support the theoretical results.

Contents

1 Introduction

Fractional step methods for the incompressible Navier-Stokes equations have enjoyed widespread popularity since the original works of Chorin [1] and Temam [2]. The reason for this relies of the computational efficiency of these methods (see e.g. [3, 4, 5]), basically due to the uncoupling of the pressure from the velocity components. However, several issues related to these methods still deserve further analysis, and perhaps the most salient of these are the behavior of the computed pressure near boundaries and the stability of the pressure itself.

Referring to the pressure boundary conditions, it is well known that numerical boundary layers may appear. The reason for this can be explained by considering the pressure boundary condition associated to the splitting of the continuous problem as proposed in [1, 2]. Although relevant in some cases, this misbehavior does not affect the global pressure convergence [6], and can be shown to be less dramatic than expected in most situations [7]. In any case, any reference to the correct boundary conditions for the fractional step scheme can be skipped by considering the splitting at the purely algebraic level, once the space discretization has been performed. This is the approach advocated in [8, 9] and that we will follow here.

The study of the pressure stability for schemes that use a pressure Poisson equation is the main concern of this paper. Surprisingly, this stability is rarely made explicit. It is normally hidden by the convergence analysis, when it is required that the time step size be *small enough*. In general, analyses at the continuous space level are based on the stability of the continuous pressure [10, 11], whereas when the space is discretized it relies on the stability of this dicretization, either the finite element method as in [12] or a very simple finite difference setting as in [13]. Other attempts to study the pressure stability are presented in [14], where results much weaker than those presented here are stated.

The results to be presented in this paper refer to two types of fractional step schemes, namely, the classical first order projection method and a second order algorithm based on the Crank-Nicolson discretization for the viscous and convective terms and a second order pressure splitting, leaving the pressure gradient at a given time level in the first step and computing its increment in the second one (see [15, 16, 17, 11, 18] for different ideas related to second order schemes). Firstly, the stability of these schemes in the context of a finite element space discretization is analyzed in Section 3 using matrix arguments. It is shown that a certain pressure stability can be expected, regardless of the particular discrete velocity-pressure spaces chosen. This stability can be useful for the first order scheme, but it is certainly too weak for the second order one. In both cases, though, it is given by the time step size, and hence this size is limited from below simply to stabilize the space discretization. It is worth noting that this dependence of the stabilization terms on the time step size also appears in some formulations aiming to stabilize *convection*, and not the velocity-pressure interpolation (see [19] for a version of the Characteristic-Galerkin method where this fact is clearly demonstrated).

In order to avoid the bond described, a pressure stabilized scheme is proposed in Section 4. Again, the stability analysis of both the first and second order fractional step schemes is undertaken, now using a variational setting rather than the previous matrix language. This stabilization is intended to mimic the stabilizing effect of the first order projection method. The method was originally presented in [20] for the steady Stokes problem, extended to the nonlinear case in [21] and to the transient problem using a monolithic time discretization in [22]. In spite of the fact that the variational approach used in Section 4 supersedes the matrix analysis of Section 3, the latter is extremely useful to understand the stabilization mechanism introduced by the splitting and, more precisely, by approximation (14) in Section 2.

The final step is to extend the previous stabilization method to the case in which convection needs also to be stabilized. The resulting formulation, based on the ideas of [23], is presented in Section 5. It is able to have control over the pressure gradient and the nonlinear convective term while yielding very accurate numerical results, much less overdiffusive than classical pressure stabilization methods or upwind techniques designed to deal with convection dominated flows.

Some numerical results are presented in Section 6. In spite of their simplicity, they clearly show that the theoretical predictions of the paper are encountered in practice. The summary of the most salient results and the conclusions are finally presented in Section 7.

2 Fractional step methods for the Navier-Stokes equations

2.1 Problem statement

2.1.1 Continuous problem

In the simplest possible setting, the incompressible Navier-Stokes equations for a fluid moving in a domain Ω of $\mathbb{R}^d$ ($d = 2$ or 3) in a time interval $[0, T]$ are

$$\partial_t \boldsymbol{u} + \boldsymbol{u} \cdot \nabla \boldsymbol{u} - \nu \Delta \boldsymbol{u} + \nabla p = \boldsymbol{f} \qquad \text{in } \Omega,\ t \in (0, T), \tag{1}$$

$$\nabla \cdot \boldsymbol{u} = 0 \quad \text{in } \Omega,\ t \in (0, T), \tag{2}$$

where $\boldsymbol{u}$ is the velocity field, p the kinematic pressure, $\boldsymbol{f}$ the vector field of body forces and $\nu > 0$ the kinematic viscosity. These equations need to be supplied with an initial condition for the velocity and a boundary condition, which, for simplicity, we will take as the simple homogeneous Dirichlet condition $\boldsymbol{u} = \boldsymbol{0}$ on $\partial\Omega$, $t \in [0, T]$.

The finite element space discretization that we will consider is based on the variational formulation of the problem. In order to write it, let us introduce the forms

$$a(\boldsymbol{u}, \boldsymbol{v}) := \nu(\nabla \boldsymbol{u}, \nabla \boldsymbol{v}), \quad b(q, \boldsymbol{v}) := (q, \nabla \cdot \boldsymbol{u}),$$

$$c(\boldsymbol{u}, \boldsymbol{v}, \boldsymbol{w}) := (\boldsymbol{u} \cdot \nabla \boldsymbol{v}, \boldsymbol{w}) + \frac{1}{2}\left((\nabla \cdot \boldsymbol{u})\boldsymbol{v}, \boldsymbol{w}\right),$$

where $(\cdot,\cdot)$ denotes the standard L^2 inner product. In these expressions, for a fixed $t \in [0,T]$, $\boldsymbol{u}, \boldsymbol{v}, \boldsymbol{w}$ are assumed to belong to the velocity space $\boldsymbol{V} = [H_0^1(\Omega)]^d$ of vector functions whose components and their derivatives are square-integrable and vanish on $\partial\Omega$, and q belongs to the pressure space $Q = L^2(\Omega)/\mathbb{R}$ of square-integrable functions modulo constants. Observe that c corresponds to the skew-symmetric form of the convective term. For exactly divergence free $\boldsymbol{u}$, the second term of c vanishes. However, it will simplify the analysis of the discrete problem, where we will often make use of the property $c(\boldsymbol{u}, \boldsymbol{v}, \boldsymbol{v}) = 0$ for all $\boldsymbol{v} \in \boldsymbol{V}$.

Having introduced this notation, the weak form of problem (1)-(2) consists of finding $\boldsymbol{u}$ and p such that

$$
\begin{aligned}
&(\partial_t \boldsymbol{u}, \boldsymbol{v}) + c(\boldsymbol{u}, \boldsymbol{u}, \boldsymbol{v}) + a(\boldsymbol{u}, \boldsymbol{v}) - b(p, \boldsymbol{v}) = \langle \boldsymbol{f}, \boldsymbol{v} \rangle \quad \forall \boldsymbol{v} \in \boldsymbol{V}, \\
&b(q, \boldsymbol{u}) = 0 \quad \forall q \in Q,
\end{aligned}
$$

and $\boldsymbol{u}$ satisfying the initial condition. The notation $\langle \boldsymbol{f}, \boldsymbol{v} \rangle$ stands for the duality pairing of $\boldsymbol{v} \in \boldsymbol{V}$ and $\boldsymbol{f} \in [H^{-1}(\Omega)]^d$ (for $t \in [0,T]$).

2.1.2 Monolithic time discretization

We start by considering the simplest time discretization of the problem, namely, the trapezoidal rule. Let $\theta \in [0,1]$ be a given parameter and consider a partition of $[0,T]$ into N time steps of (for simplicity) equal size δt. Let f be a generic function of time and f^n the value of f at $t^n = n\delta t$ or an approximation to it, and let $f^{n+\theta} := \theta f^{n+1} + (1-\theta) f^n$, $\delta_t f^n := (f^{n+1} - f^n)/\delta t$. Given $\boldsymbol{u}^n$ at t^n, the time discrete problem consists of finding $\boldsymbol{u}^{n+1}$ and p^{n+1} at t^{n+1} as the solution of

$$
(\delta_t \boldsymbol{u}^n, \boldsymbol{v}) + c(\boldsymbol{u}^{n+\theta}, \boldsymbol{u}^{n+\theta}, \boldsymbol{v}) + a(\boldsymbol{u}^{n+\theta}, \boldsymbol{v}) - b(p^{n+1}, \boldsymbol{v}) = \langle \boldsymbol{f}^{n+\theta}, \boldsymbol{v} \rangle \quad \forall \boldsymbol{v} \in \boldsymbol{V}, \tag{3}
$$

$$
b(q, \boldsymbol{u}^{n+1}) = 0 \quad \forall q \in Q. \tag{4}
$$

The pressure value computed here has been identified as the pressure evaluated at t^{n+1}, although this is irrelevant for the velocity approximation. The values of interest of θ are $\theta = 1/2$, corresponding to the second order Crank-Nicolson scheme (see [24] for a thorough analysis of this scheme) and $\theta = 1$, which corresponds to the backward Euler method. If $\boldsymbol{f}$ is not continuous in time, $\langle \boldsymbol{f}^{n+\theta}, \boldsymbol{v} \rangle$ can be taken as the time average of $\langle \boldsymbol{f}, \boldsymbol{v} \rangle$ over the time step $[t^n, t^{n+1}]$.

2.1.3 Finite element discretizations

Let $\boldsymbol{V}_h$ be a finite element space to approximate $\boldsymbol{V}$ and Q_h a finite element approximation to Q. Functions in $\boldsymbol{V}_h$ need to be continuous piecewise polynomials, whereas continuity is in principle not required for Q_h. However, we will consider only continuous pressure interpolations, for reasons explained below.

The finite element discretization of (3)-(4) reads:

$$(\delta_t \boldsymbol{u}_h^n, \boldsymbol{v}_h) + c(\boldsymbol{u}_h^{n+\theta}, \boldsymbol{u}_h^{n+\theta}, \boldsymbol{v}_h) + a(\boldsymbol{u}_h^{n+\theta}, \boldsymbol{v}_h) - b(p_h^{n+1}, \boldsymbol{v}_h) = \langle \boldsymbol{f}^{n+1}, \boldsymbol{v}_h \rangle \quad \forall \boldsymbol{v}_h \in \boldsymbol{V}_h,$$
$$b(q_h, \boldsymbol{u}_h^{n+1}) = 0 \quad \forall q_h \in Q_h.$$

It is well known that for this discrete problem to be stable the velocity and pressure spaces need to satisfy the classical inf-sup condition (see e.g. [25]), which in particular precludes the use of convenient *equal* velocity-pressure interpolations. However, it was early noted that this condition is not required when fractional step methods using a pressure Poisson equation are employed (see e.g. [26, 27, 28, 29]). *The analysis and clarification of this situation is precisely the objective of this paper.*

Before presenting the fractional step schemes to be studied, let us introduce the matrix form of the problem. This is given by

$$\mathsf{M}\delta_t \mathsf{U}^n + \mathsf{K}(\mathsf{U}^{n+\theta})\mathsf{U}^{n+\theta} + \mathsf{G}\mathsf{P}^{n+1} = \mathsf{F}^{n+\theta}, \tag{5}$$
$$\mathsf{D}\mathsf{U}^{n+1} = \mathsf{0}, \tag{6}$$

where U and P are the arrays of nodal velocities and pressures, respectively. If we denote the node indexes with superscripts a, b, the space indexes with subscripts i, j, and the standard shape function of node a by N^a, the components of the arrays involved in these equations are:

$$\mathsf{M}_{ij}^{ab} = (N^a, N^b)\delta_{ij} \quad (\delta_{ij} \text{ is the Kronecker } \delta),$$
$$\mathsf{K}(\mathsf{U}^{n+\theta})_{ij}^{ab} = (N^a, \boldsymbol{u}_h^{n+\theta} \cdot \nabla N^b)\delta_{ij} + \frac{1}{2}\left(N^a, (\nabla \cdot \boldsymbol{u}_h^{n+\theta}) N^b\right)\delta_{ij} + \nu(\nabla N^a, \nabla N^b)\delta_{ij},$$
$$\mathsf{G}_i^{ab} = -(\partial_i N^a, N^b),$$
$$\mathsf{F}_i^a = \langle N^a, f_i \rangle,$$
$$\mathsf{D}_j^{ab} = (N^a, \partial_j N^b).$$

It is understood that all the arrays are matrices (except F, which is a vector) whose components are obtained by grouping together the left indexes in the previous expressions (a and possibly i) and the right indexes (b and possibly j).

2.2 Fractional step schemes

The fractional step schemes we will consider can be introduced at this point, applied to the fully discrete problem (5)-(6). This is exactly equivalent to

$$\mathsf{M}\frac{1}{\delta t}(\hat{\mathsf{U}}^{n+1} - \mathsf{U}^n) + \mathsf{K}(\mathsf{U}^{n+\theta})\mathsf{U}^{n+\theta} + \gamma \mathsf{G}\mathsf{P}^n = \mathsf{F}^{n+\theta}, \tag{7}$$
$$\mathsf{M}\frac{1}{\delta t}(\mathsf{U}^{n+1} - \hat{\mathsf{U}}^{n+1}) + \mathsf{G}(\mathsf{P}^{n+1} - \gamma \mathsf{P}^n) = \mathsf{0}, \tag{8}$$
$$\mathsf{D}\mathsf{U}^{n+1} = \mathsf{0}, \tag{9}$$

where $\hat{\mathsf{U}}^{n+1}$ is an auxiliary variable and γ is a numerical parameter, whose values of interest are 0 and 1. At this point we can make the essential approximation

$$\mathsf{K}(\mathsf{U}^{n+\theta})\mathsf{U}^{n+\theta} \approx \mathsf{K}(\hat{\mathsf{U}}^{n+\theta})\hat{\mathsf{U}}^{n+\theta}, \tag{10}$$

where $\hat{\mathsf{U}}^{n+\theta} := \theta\hat{\mathsf{U}}^{n+1} + (1-\theta)\mathsf{U}^n$. Expressing U^{n+1} in terms of $\hat{\mathsf{U}}^{n+1}$ using (8) and inserting the result in (9), the set of equations to be solved is

$$\mathsf{M}\frac{1}{\delta t}(\hat{\mathsf{U}}^{n+1} - \mathsf{U}^n) + \mathsf{K}(\hat{\mathsf{U}}^{n+\theta})\hat{\mathsf{U}}^{n+\theta} + \gamma\mathsf{G}\mathsf{P}^n = \mathsf{F}^{n+\theta}, \tag{11}$$

$$\delta t\,\mathsf{D}\mathsf{M}^{-1}\mathsf{G}(\mathsf{P}^{n+1} - \gamma\mathsf{P}^n) = \mathsf{D}\hat{\mathsf{U}}^{n+1}, \tag{12}$$

$$\mathsf{M}\frac{1}{\delta t}(\mathsf{U}^{n+1} - \hat{\mathsf{U}}^{n+1}) + \mathsf{G}(\mathsf{P}^{n+1} - \gamma\mathsf{P}^n) = \mathsf{0}, \tag{13}$$

which have been ordered according to the sequence of solution, for $\hat{\mathsf{U}}^{n+1}$, P^{n+1} and U^{n+1}. This uncoupling of variables has been made possible by (10). This approximation is interpreted in [8, 9] as an *incomplete block LU factorization* of the original problem (7)-(9). The advantage of this discrete approach is that now there is no question about the boundary conditions for the intermediate variable $\hat{\mathsf{U}}^{n+1}$: since boundary conditions are incorporated in the discrete problem (5)-(6), the prescriptions for $\hat{\mathsf{U}}^{n+1}$ are exactly the same as for the end-of-step velocity U^{n+1}.

Even though problem (11)-(13) can be implemented as such, it is very convenient to make a further approximation. Observe that $\mathsf{D}\mathsf{M}^{-1}\mathsf{G}$ represents an approximation to the Laplacian operator. In order to avoid dealing with this matrix (which is computationally feasible only if M is approximated by a diagonal matrix), we can approximate

$$\mathsf{D}\mathsf{M}^{-1}\mathsf{G} \approx \mathsf{L}, \quad \text{with components } \mathsf{L}^{ab} = -(\nabla N^a, \nabla N^b). \tag{14}$$

Matrix L is the standard approximation to the Laplacian operator. The quality of approximation (14) is discussed bellow. Clearly, this approximation is only possible when continuous pressure interpolations are employed.

After using (10) and (14) the problem to be solved is:

$$\mathsf{M}\frac{1}{\delta t}(\hat{\mathsf{U}}^{n+1} - \mathsf{U}^n) + \mathsf{K}(\hat{\mathsf{U}}^{n+\theta})\hat{\mathsf{U}}^{n+\theta} + \gamma\mathsf{G}\mathsf{P}^n = \mathsf{F}^{n+\theta}, \tag{15}$$

$$\delta t\,\mathsf{L}(\mathsf{P}^{n+1} - \gamma\mathsf{P}^n) = \mathsf{D}\hat{\mathsf{U}}^{n+1}, \tag{16}$$

$$\mathsf{M}\frac{1}{\delta t}(\mathsf{U}^{n+1} - \hat{\mathsf{U}}^{n+1}) + \mathsf{G}(\mathsf{P}^{n+1} - \gamma\mathsf{P}^n) = \mathsf{0}. \tag{17}$$

Once arrived at this point, we may also write the discrete variational equations corresponding to this matrix problem, which are

$$\begin{aligned}
&\frac{1}{\delta t}(\hat{\boldsymbol{u}}_h^{n+1} - \boldsymbol{u}_h^n, \boldsymbol{v}_h) + c(\hat{\boldsymbol{u}}_h^{n+\theta}, \hat{\boldsymbol{u}}_h^{n+\theta}, \boldsymbol{v}_h) + a(\hat{\boldsymbol{u}}_h^{n+\theta}, \boldsymbol{v}_h) - \gamma b(p_h^n, \boldsymbol{v}_h) \\
&\qquad = \langle \boldsymbol{f}^{n+1}, \boldsymbol{v}_h \rangle \quad \forall \boldsymbol{v}_h \in \boldsymbol{V}_h, \\
&-\delta t\,(\nabla(p_h^{n+1} - \gamma p_h^n), \nabla q_h) = (q_h, \nabla \cdot \hat{\boldsymbol{u}}_h^{n+1}) \quad \forall q_h \in Q_h, \\
&\frac{1}{\delta t}(\boldsymbol{u}_h^{n+1} - \hat{\boldsymbol{u}}_h^{n+1}, \boldsymbol{v}_h) - b(p_h^{n+1} - \gamma p_h^n, \boldsymbol{v}_h) = 0 \quad \forall \boldsymbol{v}_h \in \boldsymbol{V}_h,
\end{aligned}$$

where $\hat{\boldsymbol{u}}_h$ is obviously the piecewise continuous function obtained by interpolating from the nodal values $\hat{\mathsf{U}}$.

Formally, it is easy to see that the splitting error, introduced by approximation (10), is of order $O(\delta t)$ when $\gamma = 0$ and of order $O(\delta t^2)$ when $\gamma = 1$ (observe from (17) that $O(\|\mathsf{U}^{n+1} - \hat{\mathsf{U}}^{n+1}\|) = \delta t\, O(\|\mathsf{P}^{n+1} - \gamma \mathsf{P}^n\|)$ in any norm $\|\cdot\|$). In order to have the same error due to the splitting and due to the original time discretization, we will consider two sets of parameters. The first is $\gamma = 0$, $\theta = 1$, which yields the classical first order projection scheme, and the second $\gamma = 1$, $\theta = 1/2$, which yields a (formally) second order time accurate method.

3 Basic stability estimates

In this section we obtain stability estimates for the two schemes described above. We show that there is a certain pressure stability *regardless of any compatibility requirement between the velocity and pressure approximations*. In order to understand how is this possible, we show first how the fractional step scheme (15)-(17) can be viewed as a *stabilized* monolithic scheme.

3.1 Equivalent stabilized monolithic formulations

In problem (15)-(17) we can eliminate either $\hat{\mathsf{U}}$ or U, and think of the remaining variable as the approximation to the velocity. These two possibilities lead to two different stabilized formulations, as we show now.

Let us start by writing the problem only in terms of $\hat{\mathsf{U}}$. Since

$$\mathsf{U}^n = \hat{\mathsf{U}}^n - \delta t\, \mathsf{M}^{-1}\mathsf{G}(\mathsf{P}^n - \gamma \mathsf{P}^{n-1}),$$

equations (15)-(17) can be re-written as

$$\mathsf{M}\frac{1}{\delta t}(\hat{\mathsf{U}}^{n+1} - \hat{\mathsf{U}}^n) + \mathsf{K}(\hat{\mathsf{U}}^{n+\theta})\hat{\mathsf{U}}^{n+\theta} + \mathsf{G}[(1+\gamma)\mathsf{P}^n - \gamma \mathsf{P}^{n-1}] = \mathsf{F}^{n+1}, \tag{18}$$

$$\mathsf{D}\hat{\mathsf{U}}^{n+1} - \delta t\, \mathsf{L}(\mathsf{P}^{n+1} - \gamma \mathsf{P}^n) = \mathsf{0}. \tag{19}$$

In the case $\gamma = 0$, this formulation can be viewed as a *stabilized* finite element method, the stabilization effect coming from the pressure Laplacian in the discrete continuity equation (19), in a similar way to other popular methods such as Galerkin/Least-Squares [30, 31, 32]. Except for the parameter multiplying L, which now is δt, the formulation is similar to the stabilization method analyzed in [33]. This observation was first pointed out in [34]. Let us remark that the use of $\hat{\mathsf{U}}$ as the velocity variable is also proposed in [35].

An additional comment is that, even though the pressure gradient is treated explicitly in (18), the resulting scheme turns out to be *stable* in time. This results from the forthcoming analysis.

A different approach was advocated in [28]. The idea is to write the problem in terms of U rather than $\hat{\mathsf{U}}$. Since

$$\hat{\mathsf{U}}^{n+1} = \mathsf{U}^{n+1} + \delta t\, \mathsf{M}^{-1}\mathsf{G}(\mathsf{P}^{n+1} - \gamma \mathsf{P}^n), \tag{20}$$

equations (15)-(17) can be also re-written as

$$\begin{aligned} &\mathsf{M}\frac{1}{\delta t}(\mathsf{U}^{n+1} - \mathsf{U}^n) + \mathsf{K}(\mathsf{U}^{n+\theta})\mathsf{U}^{n+\theta} + \mathsf{E}(\mathsf{U}^{n+\theta}) + \mathsf{G}\mathsf{P}^{n+1} = \mathsf{F}^{n+1}, \\ &\mathsf{D}\mathsf{U}^{n+1} + \delta t\,(\mathsf{D}\mathsf{M}^{-1}\mathsf{G} - \mathsf{L})(\mathsf{P}^{n+1} - \gamma \mathsf{P}^n) = \mathsf{0}, \end{aligned} \tag{21}$$

where $\mathsf{E}(\mathsf{U}^{n+\theta})$ can be thought of as the splitting error, and is given by

$$\begin{aligned} &\mathsf{E}(\mathsf{U}^{n+\theta}) := \mathsf{K}(\mathsf{S}^{n+\theta})\mathsf{U}^{n+\theta} + \mathsf{K}(\mathsf{U}^{n+\theta})\mathsf{S}^{n+\theta} + \mathsf{K}(\mathsf{S}^{n+\theta})\mathsf{S}^{n+\theta}, \\ &\mathsf{S}^{n+\theta} := \theta\delta t\, \mathsf{M}^{-1}\mathsf{G}(\mathsf{P}^{n+1} - \gamma \mathsf{P}^n). \end{aligned}$$

Clearly, $\mathsf{E}(\mathsf{U}^{n+\theta})$ is formally of order $O(\delta t^{\,1+\gamma})$.

Consider again the case $\gamma = 0$ (what happens when $\gamma = 1$ is analyzed later). The stabilization effect now comes from the term $\delta t\, \mathsf{B}\mathsf{P}^{n+1}$, where $\mathsf{B} := \mathsf{D}\mathsf{M}^{-1}\mathsf{G} - \mathsf{L}$. It is shown in [36] that this matrix is *positive semi-definite*. For completeness, let us provide the (simple) proof here. This will allow us to introduce some of the concepts used in Section 4.

Let us consider the vector space $\boldsymbol{E}_h := \boldsymbol{V}_h + \nabla Q_h$, where ∇Q_h denotes the space of vector functions which are gradients of functions in Q_h. If n_1 is the dimension of $\boldsymbol{V}_h$ and $n_1 + n_{23}$ the dimension of $\boldsymbol{E}_h$, it can be split as

$$\boldsymbol{E}_h = \boldsymbol{V}_h \oplus \boldsymbol{V}_h^{\perp} = \mathrm{Span}\{\boldsymbol{v}_1, ..., \boldsymbol{v}_{n_1}\} \oplus \mathrm{Span}\{\boldsymbol{v}'_1, ..., \boldsymbol{v}'_{n_{23}}\}.$$

Let q_h be an arbitrary element in Q_h and Q the array of nodal values of q_h, and consider the decomposition

$$\nabla q_h = \boldsymbol{\pi}_1 + \boldsymbol{\pi}_{23} = \sum_{k=1}^{n_1} \Pi_{1,k}\boldsymbol{v}_k + \sum_{k=1}^{n_{23}} \Pi_{23,k}\boldsymbol{v}'_k, \qquad \boldsymbol{\pi}_1 \in \boldsymbol{V}_h,\ \boldsymbol{\pi}_{23} \in \boldsymbol{V}_h^{\perp},$$

where Π_1 and Π_{23} are the arrays of nodal values of $\boldsymbol{\pi}_1$ and $\boldsymbol{\pi}_{23}$, respectively. We have that

$$-\mathsf{Q}\cdot\mathsf{L}\mathsf{Q} = \int_\Omega |\nabla q_h|^2\, \mathrm{d}\Omega = \Pi_1 \cdot \mathsf{M}\Pi_1 + \int_\Omega \boldsymbol{\pi}_{23}\cdot\boldsymbol{\pi}_{23}\, \mathrm{d}\Omega,$$

and, on the other hand, if M^{-1}_{ij} are the components of M^{-1}:

$$\begin{aligned} \mathsf{Q}\cdot\mathsf{D}\mathsf{M}^{-1}\mathsf{G}\mathsf{Q} &= -\sum_{i,j=1}^{n_1} \left(\int_\Omega \nabla q_h \cdot \boldsymbol{v}_i\, \mathrm{d}\Omega\right) \mathsf{M}^{-1}_{ij} \left(\int_\Omega \nabla q_h \cdot \boldsymbol{v}_j\, \mathrm{d}\Omega\right) \\ &= -\sum_{i,j=1}^{n_1}\sum_{k,l=1}^{n_1} \Pi_{1,k} \left(\int_\Omega \boldsymbol{v}_k \cdot \boldsymbol{v}_i\, \mathrm{d}\Omega\right) \mathsf{M}^{-1}_{ij} \Pi_{1,l} \left(\int_\Omega \boldsymbol{v}_l \cdot \boldsymbol{v}_j\, \mathrm{d}\Omega\right) \\ &= -\Pi_1 \cdot \mathsf{M}\Pi_1. \end{aligned}$$

Therefore,

$$\mathsf{Q}\cdot\mathsf{BQ}=\int_\Omega \boldsymbol{\pi}_{23}\cdot\boldsymbol{\pi}_{23}\,\mathrm{d}\Omega\geq 0.$$

This proves that B is positive semi-definite and explicitly shows that the components of ∇q_h controlled by this matrix are those orthogonal to the finite element space $\boldsymbol{V}_h$, that is, $\boldsymbol{\pi}_{23}$. This fact is used in [20] to prove that approximation (14) yields an error of the same order as the pressure interpolation error, and thus it does not deteriorate the accuracy of the finite element approximation.

At this point, it is convenient to introduce some additional notation. If X, Y are arrays, $\{\mathsf{X}^n\}_{n=0,1,...,N}$ is a sequence of arrays of $N+1$ terms and A a symmetric positive semi-definite matrix, we define

$$\begin{aligned}
&\|\mathsf{X}\|_{\mathsf{A}}:=(\mathsf{X}\cdot\mathsf{AX})^{1/2},\\
&\|\mathsf{Y}\|_{-\mathsf{A}}:=\sup_{\mathsf{X}\neq\mathsf{0}}\frac{\mathsf{Y}\cdot\mathsf{X}}{\|\mathsf{X}\|_{\mathsf{A}}}\quad\text{(here }\mathsf{A}\text{ is assumed to be positive definite)},\\
&\{\mathsf{X}^n\}\in\ell^\infty(\mathsf{A})\iff\|\mathsf{X}^n\|_{\mathsf{A}}<\infty\quad\forall\, n=0,1,...,N,\\
&\{\mathsf{X}^n\}\in\ell^p(\mathsf{A})\iff\sum_{n=0}^{N}\delta t\,\|\mathsf{X}^n\|_{\mathsf{A}}^p<\infty,\quad 1\leq p<\infty.
\end{aligned}$$

A remark is needed when $\mathsf{A}=\mathsf{K}$. This matrix is not symmetric, but it has the contribution from the convective term, which is skew-symmetric, and the contribution from the viscous term, $\mathsf{K}_{\rm visc}$, which is symmetric and positive-definite. We will simply write $\mathsf{U}\cdot\mathsf{K}(\mathsf{U})\mathsf{U}=\mathsf{U}\cdot\mathsf{K}_{\rm visc}\mathsf{U}\equiv\|\mathsf{U}\|_{\mathsf{K}}^2$.

We will make use also of $\mathsf{L}^+:=-\mathsf{L}$, which is the positive semi-definite matrix corresponding to the discretization of $-\Delta$.

These definitions will allow us to express our stability results in a compact manner. The basic assumption in all the cases will be that

$$\sum_{n=0}^{N}\delta t\,\|\mathsf{F}^n\|_{-\mathsf{K}}^2\leq C<\infty,\tag{22}$$

which is the matrix version of the classical condition required for the problem to be well posed. Here and in the following, C denotes a positive constant, not necessarily the same at different appearances.

3.2 Stability of the first order projection method

We will study now the stability properties of the first order projection method, which corresponds to scheme (15)-(17) with $\gamma=0$ and $\theta=1$:

$$\mathsf{M}\frac{1}{\delta t}(\hat{\mathsf{U}}^{n+1}-\mathsf{U}^n)+\mathsf{K}(\hat{\mathsf{U}}^{n+1})\hat{\mathsf{U}}^{n+1}=\mathsf{F}^{n+1},\tag{23}$$

$$\delta t\,\mathsf{LP}^{n+1}=\mathsf{D}\hat{\mathsf{U}}^{n+1},\tag{24}$$

$$\mathsf{M}\frac{1}{\delta t}(\mathsf{U}^{n+1}-\hat{\mathsf{U}}^{n+1})+\mathsf{GP}^{n+1}=\mathsf{0}.\tag{25}$$

The stability result for this scheme reads:

Stability of the first order projection scheme:

$$\{\mathsf{U}^n\} \in \ell^\infty(\mathsf{M}), \quad \{\hat{\mathsf{U}}^n\} \in \ell^\infty(\mathsf{M}) \cap \ell^2(\mathsf{K}), \quad \{\sqrt{\delta t}\,\mathsf{P}^n\} \in \ell^2(\mathsf{L}^+)$$

To prove the result, let us multiply (23) by $2\delta t\,\hat{\mathsf{U}}^{n+1}$ and (25) by $2\delta t\,\mathsf{U}^{n+1}$. Using the relation $2a(a-b) = a^2 - b^2 + (a-b)^2$ it is easily obtained that

$$\|\hat{\mathsf{U}}^{n+1}\|^2_{\mathsf{M}} - \|\mathsf{U}^n\|^2_{\mathsf{M}} + \|\hat{\mathsf{U}}^{n+1} - \mathsf{U}^n\|^2_{\mathsf{M}} + \delta t\,\|\hat{\mathsf{U}}^{n+1}\|^2_{\mathsf{K}} \le \delta t\,\|\mathsf{F}^{n+1}\|^2_{-\mathsf{K}}, \tag{26}$$

$$\|\mathsf{U}^{n+1}\|^2_{\mathsf{M}} - \|\hat{\mathsf{U}}^{n+1}\|^2_{\mathsf{M}} + \|\mathsf{U}^{n+1} - \hat{\mathsf{U}}^{n+1}\|^2_{\mathsf{M}} + 2\delta t\,\mathsf{U}^{n+1}\cdot\mathsf{G}\mathsf{P}^{n+1} = 0. \tag{27}$$

On the other hand, from (24) multiplied by P^{n+1}, using the fact that $\mathsf{G} = -\mathsf{D}^{\mathrm{t}}$, and (20) with $\gamma = 0$, we have

$$\delta t\,\mathsf{P}^{n+1}\cdot\mathsf{L}\mathsf{P}^{n+1} = -\mathsf{U}^{n+1}\cdot\mathsf{G}\mathsf{P}^{n+1} + \delta t\,\mathsf{P}^{n+1}\cdot\mathsf{D}\mathsf{M}^{-1}\mathsf{G}\mathsf{P}^{n+1},$$

$$2\delta t\,\mathsf{U}^{n+1}\cdot\mathsf{G}\mathsf{P}^{n+1} = 2\delta t^2\,\mathsf{P}^{n+1}\cdot\mathsf{B}\mathsf{P}^{n+1} = 2\delta t\,\|\sqrt{\delta t}\,\mathsf{P}^{n+1}\|^2_{\mathsf{B}}.$$

Using this in (27), adding up (26) and (27) and summing for n (up to any $m \le N$) it follows that:

$$\{\mathsf{U}^n\} \in \ell^\infty(\mathsf{M}), \quad \{\hat{\mathsf{U}}^n\} \in \ell^2(\mathsf{K}), \quad \{\sqrt{\delta t}\,\mathsf{P}^n\} \in \ell^2(\mathsf{B}).$$

On the other hand, (25) implies

$$\|\mathsf{U}^{n+1} - \hat{\mathsf{U}}^{n+1}\|^2_{\mathsf{M}} = -\delta t^2\,\mathsf{P}^{n+1}\cdot\mathsf{D}\mathsf{M}^{-1}\mathsf{G}\mathsf{P}^{n+1},$$

and from the definition of B it is easy to see that

$$\sum_{n=0}^{N}\delta t\,\|\sqrt{\delta t}\,\mathsf{P}^{n+1}\|^2_{\mathsf{L}^+} = \sum_{n=0}^{N}\delta t^2\,\mathsf{P}^{n+1}\cdot\mathsf{B}\mathsf{P}^{n+1} + \sum_{n=0}^{N}\|\mathsf{U}^{n+1} - \hat{\mathsf{U}}^{n+1}\|^2_{\mathsf{M}}.$$

Both terms on the right-hand-side are bounded. The first because because $\{\sqrt{\delta t}\,\mathsf{P}^n\} \in \ell^2(\mathsf{B})$, and the second because it is part of the contribution from (27) when it is added up with (26) and summed for n. Therefore,

$$\{\sqrt{\delta t}\,\mathsf{P}^n\} \in \ell^2(\mathsf{L}^+).$$

It remains to show that $\{\hat{\mathsf{U}}^n\} \in \ell^\infty(\mathsf{M})$, which follows easily adding up (26) and (27) evaluated at n instead of $n+1$ and summing for n.

3.3 Stability of the second order scheme

The second order scheme corresponds to the choices $\gamma = 1$ and $\theta = 1/2$ in (15)-(17), that is,

$$\mathsf{M}\frac{1}{\delta t}(\hat{\mathsf{U}}^{n+1} - \mathsf{U}^n) + \mathsf{K}(\hat{\mathsf{U}}^{n+1/2})\hat{\mathsf{U}}^{n+1/2} + \mathsf{G}\mathsf{P}^n = \mathsf{F}^{n+1/2}, \tag{28}$$

$$\delta t\,\mathsf{L}(\mathsf{P}^{n+1} - \mathsf{P}^n) = \mathsf{D}\hat{\mathsf{U}}^{n+1}, \tag{29}$$

$$\mathsf{M}\frac{1}{\delta t}(\mathsf{U}^{n+1} - \hat{\mathsf{U}}^{n+1}) + \mathsf{G}(\mathsf{P}^{n+1} - \mathsf{P}^n) = 0. \tag{30}$$

We will take $\mathsf{P}^0 = \mathsf{0}$. For this method, the stability result is:

Stability of the second order scheme:

$$\{\mathsf{U}^n\} \in \ell^\infty(\mathsf{M}), \quad \{\hat{\mathsf{U}}^n\} \in \ell^\infty(\mathsf{M}), \quad \{\hat{\mathsf{U}}^{n+1/2}\} \in \ell^2(\mathsf{K}),$$

$$\{\delta t\, \mathsf{P}^n\} \in \ell^\infty(\mathsf{L}^+), \quad \{\sqrt{\delta t}\, \delta \mathsf{P}^n\} \in \ell^2(\mathsf{L}^+)$$

Let us prove this. Multiplying (28) by $2\delta t\, \hat{\mathsf{U}}^{n+1/2} = \delta t\, (\hat{\mathsf{U}}^{n+1} + \mathsf{U}^n)$ and (30) by $\delta t\, (\mathsf{U}^{n+1} + \hat{\mathsf{U}}^{n+1})$ it is found that

$$\begin{aligned} &\|\hat{\mathsf{U}}^{n+1}\|_{\mathsf{M}}^2 - \|\mathsf{U}^n\|_{\mathsf{M}}^2 + \delta t\, \|\hat{\mathsf{U}}^{n+1/2}\|_{\mathsf{K}}^2 + \delta t\, (\hat{\mathsf{U}}^{n+1} + \mathsf{U}^n)\mathsf{G}\mathsf{P}^n \leq C\delta t\, \|\mathsf{F}^{n+1}\|_{-\mathsf{K}}^2, \\ &\|\mathsf{U}^{n+1}\|_{\mathsf{M}}^2 - \|\hat{\mathsf{U}}^{n+1}\|_{\mathsf{M}}^2 + \delta t\, (\mathsf{U}^{n+1} + \hat{\mathsf{U}}^{n+1}) \cdot \mathsf{G}(\mathsf{P}^{n+1} - \mathsf{P}^n) = \mathsf{0}. \end{aligned} \tag{31}$$

Adding up these two expressions we find that

$$\begin{aligned} &\|\mathsf{U}^{n+1}\|_{\mathsf{M}}^2 - \|\mathsf{U}^n\|_{\mathsf{M}}^2 + \delta t\, \|\hat{\mathsf{U}}^{n+1/2}\|_{\mathsf{K}}^2 + \delta t\, \hat{\mathsf{U}}^{n+1} \cdot \mathsf{G}\mathsf{P}^{n+1} \\ &\quad + \delta t\, \mathsf{U}^n \cdot \mathsf{G}\mathsf{P}^n + \delta t\, \mathsf{U}^{n+1} \cdot \mathsf{G}\delta \mathsf{P}^n \leq C\delta t\, \|\mathsf{F}^{n+1}\|_{-\mathsf{K}}^2. \end{aligned} \tag{32}$$

From (29) it is easily found that

$$\begin{aligned} \delta t\, \hat{\mathsf{U}}^{n+1} \cdot \mathsf{G}\mathsf{P}^{n+1} &= -\delta t\, \mathsf{P}^{n+1} \cdot \mathsf{D}\hat{\mathsf{U}}^{n+1} = -\delta t^2\, \mathsf{P}^{n+1} \cdot \mathsf{L}\delta \mathsf{P}^n \\ &= \frac{\delta t^2}{2} \left(\|\mathsf{P}^{n+1}\|_{\mathsf{L}^+}^2 - \|\mathsf{P}^n\|_{\mathsf{L}^+}^2 + \|\delta \mathsf{P}^n\|_{\mathsf{L}^+}^2 \right). \end{aligned} \tag{33}$$

On the other hand, (30) implies

$$\mathsf{U}^{n+1} = \hat{\mathsf{U}}^{n+1} - \delta t\, \mathsf{M}^{-1}\mathsf{G}\delta \mathsf{P}^n,$$

and therefore

$$\begin{aligned} \delta t\, \mathsf{U}^n \cdot \mathsf{G}\mathsf{P}^n &= -\delta t\, \mathsf{P}^n \cdot \mathsf{D}\mathsf{U}^n = -\delta t\, \mathsf{P}^n \cdot \mathsf{D}(\hat{\mathsf{U}}^n - \delta t\, \mathsf{M}^{-1}\mathsf{G}\delta \mathsf{P}^{n-1}) \\ &= -\delta t\, \mathsf{P}^n \cdot (\delta t\, \mathsf{L}\delta \mathsf{P}^{n-1} - \delta t\, \mathsf{D}\mathsf{M}^{-1}\mathsf{G}\delta \mathsf{P}^{n-1}) \\ &= \delta t^2\, \mathsf{P}^n \cdot \mathsf{B}\delta \mathsf{P}^{n-1} = \frac{\delta t^2}{2} \left(\|\mathsf{P}^n\|_{\mathsf{B}}^2 - \|\mathsf{P}^{n-1}\|_{\mathsf{B}}^2 + \|\delta \mathsf{P}^{n-1}\|_{\mathsf{B}}^2 \right). \end{aligned} \tag{34}$$

Likewise,

$$\begin{aligned} \delta t\, \mathsf{U}^{n+1} \cdot \mathsf{G}\delta \mathsf{P}^n &= -\delta t\, \delta \mathsf{P}^n \cdot \mathsf{D}\mathsf{U}^{n+1} = -\delta t\, \delta \mathsf{P}^n \cdot \mathsf{D}\left(\hat{\mathsf{U}}^{n+1} - \delta t\, \mathsf{M}^{-1}\mathsf{G}\delta \mathsf{P}^n \right) \\ &= -\delta t\, \delta \mathsf{P}^n \cdot \left(\delta t\, \mathsf{L}\delta \mathsf{P}^n - \delta t\, \mathsf{D}\mathsf{M}^{-1}\mathsf{G}\delta \mathsf{P}^n \right) \\ &= \delta t^2\, \delta \mathsf{P}^n \cdot \mathsf{B}\delta \mathsf{P}^n = \delta t\, \|\sqrt{\delta t}\, \delta \mathsf{P}^n\|_{\mathsf{B}}^2. \end{aligned} \tag{35}$$

Using (33)-(35) in (32), taking $\mathsf{P}^0 = \mathsf{P}^{-1} = \mathsf{0}$ and summing for n we conclude that

$$\{\mathsf{U}^n\} \in \ell^\infty(\mathsf{M}), \quad \{\hat{\mathsf{U}}^{n+1/2}\} \in \ell^2(\mathsf{K}), \quad \{\delta t\, \mathsf{P}^n\} \in \ell^\infty(\mathsf{L}^+), \quad \{\sqrt{\delta t}\, \delta \mathsf{P}^n\} \in \ell^2(\mathsf{L}^+).$$

It remains to show that $\{\hat{\mathsf{U}}^n\} \in \ell^\infty(\mathsf{M})$. From (29) we have that

$$\delta t\, \hat{\mathsf{U}}^{n+1} \cdot \mathsf{G}\delta\mathsf{P}^n = -\delta t\, \delta\mathsf{P}^n \mathsf{D}\hat{\mathsf{U}}^{n+1} = \delta t^2 \, \|\delta\mathsf{P}^n\|^2_{\mathsf{L}^+},$$

which substituted in (31) yields, after making use of (35),

$$\|\hat{\mathsf{U}}^{n+1}\|^2_{\mathsf{M}} = \|\mathsf{U}^{n+1}\|^2_{\mathsf{M}} + \delta t^2 \, \|\delta\mathsf{P}^n\|^2_{\mathsf{L}^+} + \delta t^2 \, \|\delta\mathsf{P}^n\|^2_{\mathsf{B}}.$$

The result follows noting that all the right-hand-side terms are ℓ^∞ sequences.

4 Pressure stabilized schemes

4.1 Pressure stabilization

It has been shown in the previous section that the pressure stability of both the first and second order schemes depends on the time step size. It can be anticipated that if δt is very small stability problems may occur, especially for the second order scheme. In order to avoid this, one can resort to a *stabilized* formulation, in the same spirit as for monolithic schemes.

Since the stability of the first order scheme is known to be adequate when δt is taken close to the critical time step of the explicit scheme ($\theta = 0$ in (5)), it seems natural to devise a stabilized formulation which inherits the stabilization effect of this first order scheme. This idea was first developed in [20] for the Stokes problem, and is briefly reproduced here for the transient Navier-Stokes equations and used in conjunction with a fractional step method.

Let $\tilde{\mathsf{D}}$, $\tilde{\mathsf{M}}$ and $\tilde{\mathsf{G}}$ be the matrices with the same components as D, M and G, respectively, but letting the velocity shape functions run also over the boundary nodes. Starting with the monolithic time discretization, the stabilized formulation we consider is

$$\begin{aligned}
&\mathsf{M}\delta_t\mathsf{U}^n + \mathsf{K}(\mathsf{U}^{n+\theta})\mathsf{U}^{n+\theta} + \mathsf{G}\mathsf{P}^{n+1} = \mathsf{F}^{n+\theta},\\
&\mathsf{D}\mathsf{U}^{n+1} + \tau(\tilde{\mathsf{D}}\Pi^{n+\beta} - \mathsf{L}\mathsf{P}^{n+1}) = \mathsf{0},\\
&\tilde{\mathsf{M}}\Pi^{n+1} = \tilde{\mathsf{G}}\mathsf{P}^{n+1},
\end{aligned}$$

where Π is an auxiliary variable, which may be treated either implicitly if $\beta = 1$ or explicitly if $\beta = 0$, and τ is a stabilization parameter which depends on the local element sizes. For the sake of simplicity in the exposition, we will take the finite element meshes quasi-uniform, and thus τ will depend only on the diameter of the finite element partition h. The stability and convergence analysis dictates that it must behave as

$$\tau \leq C\frac{h^2}{\nu}$$

for viscous dominated cases (an appropriate choice for the constant is $C = 1/4$ when linear elements are used). In general, it can be taken close to the critical time step of the explicit time integration of (5)-(6) (see [20, 22] for further discussion). Nevertheless, the exact value of τ is irrelevant for our discussion.

To see that the modified monolithic problem will inherit the type of stability of the first order projection method, note that if $\beta = 1$ and Π is eliminated, the modified continuity equation is

$$\mathsf{D}\mathsf{U}^{n+1} + \tau\tilde{\mathsf{B}}\mathsf{P}^{n+1} = \mathsf{0}, \quad \tilde{\mathsf{B}} := \tilde{\mathsf{D}}\tilde{\mathsf{M}}^{-1}\tilde{\mathsf{G}} - \mathsf{L},$$

which is similar to (21) with $\gamma = 0$.

The reason for having modified matrices D, M and G to $\tilde{\mathsf{D}}$, $\tilde{\mathsf{M}}$ and $\tilde{\mathsf{G}}$, respectively, is that in this way the modified monolithic problem does not suffer from spurious pressure boundary layers, as it happens for the first order projection scheme (see [20] for the analysis of this point).

From the monolithic scheme we may use the same approximations (10) and (14) as for the non-stabilized (Galerkin) formulation to arrive to the split problem:

$$\begin{aligned}
&\mathsf{M}\frac{1}{\delta t}(\hat{\mathsf{U}}^{n+1} - \mathsf{U}^n) + \mathsf{K}(\hat{\mathsf{U}}^{n+\theta})\hat{\mathsf{U}}^{n+\theta} + \gamma\mathsf{G}\mathsf{P}^n = \mathsf{F}^{n+\theta},\\
&\delta t\,\mathsf{L}(\mathsf{P}^{n+1} - \gamma\mathsf{P}^n) + \tau(\mathsf{L}\mathsf{P}^{n+1} - \tilde{\mathsf{D}}\Pi^{n+\beta}) = \mathsf{D}\hat{\mathsf{U}}^{n+1},\\
&\mathsf{M}\frac{1}{\delta t}(\mathsf{U}^{n+1} - \hat{\mathsf{U}}^{n+1}) + \mathsf{G}(\mathsf{P}^{n+1} - \gamma\mathsf{P}^n) = \mathsf{0},\\
&\tilde{\mathsf{M}}\Pi^{n+1} = \tilde{\mathsf{G}}\mathsf{P}^{n+1}.
\end{aligned}$$

The variational statement corresponding to this matrix problem, which we will use in this section, consists of finding $\hat{\boldsymbol{u}}_h^{n+1} \in \boldsymbol{V}_h$, $p_h^{n+1} \in Q_h$, $\boldsymbol{u}_h^{n+1} \in \boldsymbol{V}_h$, and $\boldsymbol{\pi}_h^{n+1} \in \tilde{\boldsymbol{V}}_h$ such that

$$\begin{aligned}
&\frac{1}{\delta t}(\hat{\boldsymbol{u}}_h^{n+1} - \boldsymbol{u}_h^n, \boldsymbol{v}_h) + c(\hat{\boldsymbol{u}}_h^{n+\theta}, \hat{\boldsymbol{u}}_h^{n+\theta}, \boldsymbol{v}_h) + a(\hat{\boldsymbol{u}}_h^{n+\theta}, \boldsymbol{v}_h) - \gamma b(p_h^n, \boldsymbol{v}_h)\\
&\qquad = \langle \boldsymbol{f}^{n+\theta}, \boldsymbol{v}_h\rangle \quad \forall \boldsymbol{v}_h \in \boldsymbol{V}_h, \qquad (36)\\
&-\delta t\,(\nabla(p_h^{n+1} - \gamma p_h^n), \nabla q_h) - \tau(\nabla p_h^{n+1} - \boldsymbol{\pi}_h^{n+\beta}, \nabla q_h) = (q_h, \nabla\cdot\hat{\boldsymbol{u}}_h^{n+1}) \quad \forall q_h \in Q_h, \qquad (37)\\
&\frac{1}{\delta t}(\boldsymbol{u}_h^{n+1} - \hat{\boldsymbol{u}}_h^{n+1}, \boldsymbol{v}_h) - b(p_h^{n+1} - \gamma p_h^n, \boldsymbol{v}_h) = 0 \quad \forall \boldsymbol{v}_h \in \boldsymbol{V}_h, \qquad (38)\\
&(\boldsymbol{\pi}_h^{n+1}, \boldsymbol{\eta}_h) = (\nabla p_h^{n+1}, \boldsymbol{\eta}_h) \quad \forall \boldsymbol{\eta}_h \in \tilde{\boldsymbol{V}}_h, \qquad (39)
\end{aligned}$$

where $\tilde{\boldsymbol{V}}_h$ is the space $\boldsymbol{V}_h$ enlarged with the continuous vector functions associated to the boundary nodes. The meaning of the new auxiliary variable $\boldsymbol{\pi}_h$ is clearly observed from (39): it is the projection of the pressure gradient ∇p_h onto $\tilde{\boldsymbol{V}}_h$.

In the following analysis, we will need several projections of ∇p_h, all of them with respect to the L^2-inner product. These projections are

$$\begin{aligned}
&\boldsymbol{\pi}_1: \text{ projection onto } \boldsymbol{V}_h,\\
&\boldsymbol{\pi}_2: \text{ projection onto } \boldsymbol{V}_h^{\perp} \cap \tilde{\boldsymbol{V}}_h,\\
&\boldsymbol{\pi}_3: \text{ projection onto } \tilde{\boldsymbol{V}}_h^{\perp}.
\end{aligned}$$

Likewise, we will denote $\boldsymbol{\pi}_{ij} := \boldsymbol{\pi}_i + \boldsymbol{\pi}_j$. Observe in particular that $\boldsymbol{\pi}_{12} \equiv \boldsymbol{\pi}_h$, and that, using these projections, (38) implies

$$\boldsymbol{u}_h^{n+1} = \hat{\boldsymbol{u}}_h^{n+1} - \delta t\,(\boldsymbol{\pi}_1^{n+1} - \gamma\boldsymbol{\pi}_1^n). \qquad (40)$$

We will see from the following analysis that the terms multiplied by τ provide control on $\boldsymbol{\pi}_3$, that is, the component of the pressure gradient orthogonal to the space of continuous vector fields. Control on $\boldsymbol{\pi}_1$ can be directly obtained from the momentum equation, as we will see, whereas control over $\boldsymbol{\pi}_2$ follows from the condition

$$\|\nabla p_h\| \leq C(\|\boldsymbol{\pi}_1\| + \|\boldsymbol{\pi}_3\|), \tag{41}$$

which is assumed to hold for any $p_h \in Q_h$. This condition is studied in detail in [20]. In particular, it is shown to hold when equal interpolation is used for the velocity components and the pressure, the situation in which we are interested.

Similarly to Section 3, the stability estimates we will obtain here will be expressed using the following notation. Let $\{f^n\}$ be a sequence of generic functions (scalar or vectorial). We define

$$\begin{aligned}
\{f^n\} \in \ell^\infty(L^2) &\iff \|f^n\| < \infty \quad \forall\, n = 0, 1, ..., N, \\
\{f^n\} \in \ell^p(L^2) &\iff \sum_{n=0}^{N} \delta t\, \|f^n\|^p < \infty, \quad 1 \leq p < \infty, \\
\{f^n\} \in \ell^2(H^1) &\iff \sum_{n=0}^{N} \delta t\, \|f^n\|_1^2 < \infty,
\end{aligned}$$

where $\|\cdot\|$ is the standard L^2 norm and $\|\cdot\|_1$ the H^1 norm, that is, the sum of the L^2 norm of a function and the L^2 norm of its gradient. We recall that for functions f vanishing on $\partial\Omega$, $\|f\|_1$ is equivalent to $\|\nabla f\|$. Likewise, we will use the fact that $\ell^2(L^2) \subset \ell^1(L^2)$, valid for finite time intervals of analysis.

Finally, let us state the condition analogous to (22) in the variational setting that we use now, which is

$$\sum_{n=0}^{N} \delta t\, \|\boldsymbol{f}^n\|_{-1}^2 \leq C < \infty,$$

where $\|\cdot\|_{-1}$ is the dual norm of $\|\cdot\|_1$.

4.2 Stability of the stabilized first order scheme

The first order stabilized scheme is obtained taking $\gamma = 0$ and $\theta = 1$ in (36)-(39), which yields:

$$\frac{1}{\delta t}(\hat{\boldsymbol{u}}_h^{n+1} - \boldsymbol{u}_h^n, \boldsymbol{v}_h) + c(\hat{\boldsymbol{u}}_h^{n+1}, \hat{\boldsymbol{u}}_h^{n+1}, \boldsymbol{v}_h) + a(\hat{\boldsymbol{u}}_h^{n+1}, \boldsymbol{v}_h) = \langle \boldsymbol{f}^{n+1}, \boldsymbol{v}_h \rangle \quad \forall \boldsymbol{v}_h \in \boldsymbol{V}_h, \tag{42}$$

$$-\delta t\, (\nabla p_h^{n+1}, \nabla q_h) - \tau(\nabla p_h^{n+1} - \boldsymbol{\pi}_h^{n+\beta}, \nabla q_h) = (q_h, \nabla \cdot \hat{\boldsymbol{u}}_h^{n+1}) \quad \forall q_h \in Q_h, \tag{43}$$

$$\frac{1}{\delta t}(\boldsymbol{u}_h^{n+1} - \hat{\boldsymbol{u}}_h^{n+1}, \boldsymbol{v}_h) - b(p_h^{n+1}, \boldsymbol{v}_h) = 0 \quad \forall \boldsymbol{v}_h \in \boldsymbol{V}_h. \tag{44}$$

The stability result for this formulation is:

Stability of the stabilized first order scheme:

$$\{\boldsymbol{u}_h^n\} \in \ell^\infty(L^2), \quad \{\hat{\boldsymbol{u}}_h^n\} \in \ell^\infty(L^2) \cap \ell^2(H^1),$$

$$\{\sqrt{\delta t}\,\nabla p_h^n\} \in \ell^2(L^2), \quad \{\sqrt{\tau}\nabla p_h^n\} \in \ell^1(L^2)$$

Let us proceed to prove this. Taking $\boldsymbol{v}_h = 2\delta t\,\hat{\boldsymbol{u}}_h^{n+1}$ in (42) and $\boldsymbol{v}_h = 2\delta t\,\boldsymbol{u}_h^{n+1}$ in (44) it is found that

$$\|\hat{\boldsymbol{u}}_h^{n+1}\|^2 - \|\boldsymbol{u}_h^n\|^2 + \|\hat{\boldsymbol{u}}_h^{n+1} - \boldsymbol{u}_h^n\|^2 + \delta t\,\nu\|\nabla\hat{\boldsymbol{u}}_h^{n+1}\|^2 \leq C\delta t\,\|\boldsymbol{f}^{n+1}\|_{-1}^2, \tag{45}$$

$$\|\boldsymbol{u}_h^{n+1}\|^2 - \|\hat{\boldsymbol{u}}_h^{n+1}\|^2 + \|\boldsymbol{u}_h^{n+1} - \hat{\boldsymbol{u}}_h^{n+1}\|^2 - 2\delta t\,(p_h^{n+1}, \nabla\cdot\boldsymbol{u}_h^{n+1}) = 0. \tag{46}$$

On the other hand, from (43) and using (40) (with $\gamma = 0$) we have that

$$\begin{aligned}
-(p_h^{n+1}, \nabla\cdot\boldsymbol{u}_h^{n+1}) &= (\nabla p_h^{n+1}, \hat{\boldsymbol{u}}_h^{n+1}) - \delta t\,(\nabla p_h^{n+1}, \boldsymbol{\pi}_1^{n+1}) \\
&= \delta t\,(\nabla p_h^{n+1}, \nabla p_h^{n+1}) + \tau(\nabla p_h^{n+1}, \nabla p_h^{n+1} - \boldsymbol{\pi}_h^{n+\beta}) - \delta t\,(\boldsymbol{\pi}_1^{n+1}, \boldsymbol{\pi}_1^{n+1}) \\
&= \delta t\,\|\boldsymbol{\pi}_{23}^{n+1}\|^2 + \tau(\nabla p_h^{n+1}, \nabla p_h^{n+1} - \boldsymbol{\pi}_h^{n+\beta}).
\end{aligned} \tag{47}$$

Calling $\bar{\beta} := 1 - \beta$, the second term in the right-hand-side can be written as

$$\begin{aligned}
(\nabla p_h^{n+1}, \nabla p_h^{n+1} - \boldsymbol{\pi}_h^{n+\beta}) &= (\nabla p_h^{n+1}, \boldsymbol{\pi}_3^{n+1}) + \bar{\beta}(\nabla p_h^{n+1}, \boldsymbol{\pi}_h^{n+1} - \boldsymbol{\pi}_h^n) \\
&= \|\boldsymbol{\pi}_3^{n+1}\|^2 + \frac{\bar{\beta}}{2}\left(\|\boldsymbol{\pi}_h^{n+1}\|^2 - \|\boldsymbol{\pi}_h^n\|^2 + \|\boldsymbol{\pi}_h^{n+1} - \boldsymbol{\pi}_h^n\|^2\right).
\end{aligned}$$

Using this in (47), the result in (46), adding it with (45) and summing for n it is found that

$$\{\boldsymbol{u}_h^n\} \in \ell^\infty(L^2), \quad \{\hat{\boldsymbol{u}}_h^n\} \in \ell^2(H^1),$$
$$\{\sqrt{\delta t}\,\boldsymbol{\pi}_{23}^n\} \in \ell^2(L^2), \quad \{\sqrt{\tau}\boldsymbol{\pi}_3^n\} \in \ell^2(L^2).$$

On the other hand, from (40) again,

$$\|\boldsymbol{u}_h^{n+1} - \hat{\boldsymbol{u}}_h^{n+1}\|^2 = \delta t^{\,2}\|\boldsymbol{\pi}_1^{n+1}\|^2,$$

and since the sum for n of the left-hand-side is bounded (it appears when (45) and (46) are added) we have that $\{\sqrt{\delta t}\,\boldsymbol{\pi}_1^n\} \in \ell^2(L^2)$, which together with the fact that $\{\sqrt{\delta t}\,\boldsymbol{\pi}_{23}^n\} \in \ell^2(L^2)$, implies that $\{\sqrt{\delta t}\,\nabla p_h^n\} \in \ell^2(L^2)$.

Stability of $\{\sqrt{\tau}\boldsymbol{\pi}_1^n\}$ is more delicate. It is provided by the momentum equation actually solved by the fractional scheme, which after adding (42) and (44) is found to be:

$$\frac{1}{\delta t}(\boldsymbol{u}_h^{n+1} - \boldsymbol{u}_h^n, \boldsymbol{v}_h) + c(\hat{\boldsymbol{u}}_h^{n+1}, \hat{\boldsymbol{u}}_h^{n+1}, \boldsymbol{v}_h) + a(\hat{\boldsymbol{u}}_h^{n+1}, \boldsymbol{v}_h) + (\nabla p_h^{n+1}, \boldsymbol{v}_h) = \langle \boldsymbol{f}^{n+1}, \boldsymbol{v}_h\rangle.$$

Taking $\boldsymbol{v}_h = \boldsymbol{\pi}_1^{n+1}$ and using the standard inverse estimate (see e.g. [37])

$$\|\boldsymbol{\pi}_1^{n+1}\|_1 \leq \frac{C_{\text{inv}}}{h}\|\boldsymbol{\pi}_1^{n+1}\|, \tag{48}$$

valid for quasi-uniform finite element partitions, we have

$$\|\boldsymbol{\pi}_1^{n+1}\|^2 \leq \frac{1}{\delta t}\|\boldsymbol{u}_h^{n+1}-\boldsymbol{u}_h^n\|\|\boldsymbol{\pi}_1^{n+1}\| \\ +\left(N_a\|\hat{\boldsymbol{u}}_h^{n+1}\|_1+N_c\|\hat{\boldsymbol{u}}_h^{n+1}\|_1^2\right)\frac{C_{\rm inv}}{h}\|\boldsymbol{\pi}_1^{n+1}\|+\|\boldsymbol{f}^{n+1}\|_{-1}\frac{C_{\rm inv}}{h}\|\boldsymbol{\pi}_1^{n+1}\|, \tag{49}$$

where N_a and N_c are the norms of the forms a and c, respectively, and we have used the continuity of a and c, that is, $a(\boldsymbol{u},\boldsymbol{v})\leq N_a\|\boldsymbol{u}\|_1\|\boldsymbol{v}\|_1$, $c(\boldsymbol{u},\boldsymbol{v},\boldsymbol{w})\leq N_c\|\boldsymbol{u}\|_1\|\boldsymbol{v}\|_1\|\boldsymbol{w}\|_1$. Dividing by $\|\boldsymbol{\pi}_1^{n+1}\|$, summing for n, noting that $\sqrt{\tau}\leq Ch$ and using the previous stability bounds, it is found that $\{\sqrt{\tau}\boldsymbol{\pi}_1^n\}\in\ell^1(L^2)$. This, together with the fact that $\{\sqrt{\tau}\boldsymbol{\pi}_3^n\}\in\ell^2(L^2)$ and assumption (41), allows us to conclude that $\{\sqrt{\tau}\nabla p_h^n\}\in\ell^1(L^2)$. Observe that the reason why this result can not be improved to $\{\sqrt{\tau}\nabla p_h^n\}\in\ell^2(L^2)$ is the presence of the term $N_c\|\hat{\boldsymbol{u}}_h^{n+1}\|_1^2$ in (49) (see [22] for a discussion about the possibility to improve this result for the monolithic scheme).

Finally, the fact that $\{\hat{\boldsymbol{u}}_h^n\}\in\ell^\infty(L^2)$ follows adding (45) and (46) evaluated at n instead of $n+1$ and summing for n.

4.3 Stability of the stabilized second order scheme

To conclude this section, let us study the stabilized second order method, which is obtained selecting $\gamma=1$ and $\theta=1/2$ in (36)-(39):

$$\frac{1}{\delta t}(\hat{\boldsymbol{u}}_h^{n+1}-\boldsymbol{u}_h^n,\boldsymbol{v}_h)+c(\hat{\boldsymbol{u}}_h^{n+1/2},\hat{\boldsymbol{u}}_h^{n+1/2},\boldsymbol{v}_h)+a(\hat{\boldsymbol{u}}_h^{n+1/2},\boldsymbol{v}_h)-b(p_h^n,\boldsymbol{v}_h) \\ =\langle\boldsymbol{f}^{n+1/2},\boldsymbol{v}_h\rangle\quad\forall\boldsymbol{v}_h\in\boldsymbol{V}_h, \tag{50}$$

$$-\delta t\,(\nabla(p_h^{n+1}-p_h^n),\nabla q_h)-\tau(\nabla p_h^{n+1}-\boldsymbol{\pi}_h^{n+\beta},\nabla q_h)=(q_h,\nabla\cdot\hat{\boldsymbol{u}}_h^{n+1})\quad\forall q_h\in Q_h, \tag{51}$$

$$\frac{1}{\delta t}(\boldsymbol{u}_h^{n+1}-\hat{\boldsymbol{u}}_h^{n+1},\boldsymbol{v}_h)-b(p_h^{n+1}-p_h^n,\boldsymbol{v}_h)=0\quad\forall\boldsymbol{v}_h\in\boldsymbol{V}_h. \tag{52}$$

Contrary to what happened for the first order scheme, now *we need to require that* $\tau\leq C\delta t$. The stability we are able to prove in this case is:

Stability of the stabilized second order scheme:

$$\{\boldsymbol{u}_h^n\}\in\ell^\infty(L^2),\quad\{\hat{\boldsymbol{u}}_h^n\}\in\ell^\infty(L^2),\quad\{\hat{\boldsymbol{u}}_h^{n+1/2}\}\in\ell^2(H^1),$$

$$\{\delta t\,\nabla p_h^n\}\in\ell^\infty(L^2),\quad\{\sqrt{\delta t}\,\nabla\delta p_h^n\}\in\ell^2(L^2),\quad\{\sqrt{\tau}\,\nabla p_h^n\}\in\ell^1(L^2)$$

The proof-strategy is similar to the previous cases. Taking $\boldsymbol{v}_h=2\delta t\,\hat{\boldsymbol{u}}_h^{n+1/2}$ in (50) and $\boldsymbol{v}_h=\delta t\,(\boldsymbol{u}_h^{n+1}+\hat{\boldsymbol{u}}_h^{n+1})$ in (52) it is found that

$$\|\hat{\boldsymbol{u}}_h^{n+1}\|^2-\|\boldsymbol{u}_h^n\|^2+\delta t\,\nu\|\nabla\hat{\boldsymbol{u}}_h^{n+1/2}\|^2-\delta t\,(p_h^n,\nabla\cdot\hat{\boldsymbol{u}}_h^{n+1})-\delta t\,(p_h^n,\nabla\cdot\boldsymbol{u}_h^n) \\ \leq C\delta t\,\|\boldsymbol{f}^{n+1/2}\|_{-1}^2, \tag{53}$$

$$\|\boldsymbol{u}_h^{n+1}\|^2-\|\hat{\boldsymbol{u}}_h^{n+1}\|^2-\delta t\,(p_h^{n+1}-p_h^n,\nabla\cdot\boldsymbol{u}_h^{n+1})-\delta t\,(p_h^{n+1}-p_h^n,\nabla\cdot\hat{\boldsymbol{u}}_h^{n+1})=0.$$

Adding these two expressions we get

$$\|\boldsymbol{u}_h^{n+1}\|^2 - \|\boldsymbol{u}_h^n\|^2 + \delta t\,\nu\|\nabla\hat{\boldsymbol{u}}_h^{n+1/2}\|^2 - \delta t\,(p_h^n, \nabla\cdot\boldsymbol{u}_h^n) - \delta t\,(p_h^{n+1} - p_h^n, \nabla\cdot\boldsymbol{u}_h^{n+1})$$
$$-\delta t\,(p_h^{n+1}, \nabla\cdot\hat{\boldsymbol{u}}_h^{n+1}) \leq C\delta t\,\|\boldsymbol{f}^{n+1/2}\|_{-1}^2. \tag{54}$$

We need to deal with the different terms involving the pressure in the left-hand-side of this inequality. Using (51) and (52), as well as (40), the various terms can be written as

$$\begin{aligned}
-(p_h^n, \nabla\cdot\boldsymbol{u}_h^n) &= -(p_h^n, \nabla\cdot\hat{\boldsymbol{u}}_h^n) + \delta t\,(p_h^n, \nabla\cdot(\boldsymbol{\pi}_1^n - \boldsymbol{\pi}_1^{n-1})) \\
&= \delta t\,(\nabla\delta p_h^{n-1}, \nabla p_h^n) + \tau(\nabla p_h^n - \boldsymbol{\pi}_h^{n+\beta-1}, \nabla p_h^n) - \delta t\,(\nabla p_h^n, \boldsymbol{\pi}_1^n - \boldsymbol{\pi}_1^{n-1}) \\
&= \delta t\,(\boldsymbol{\pi}_{23}^n - \boldsymbol{\pi}_{23}^{n-1}, \nabla p_h^n) + \tau(\nabla p_h^n - \boldsymbol{\pi}_h^{n+\beta-1}, \nabla p_h^n) \\
&= \frac{1}{2}\delta t\,\left(\|\boldsymbol{\pi}_{23}^n\|^2 - \|\boldsymbol{\pi}_{23}^{n-1}\|^2 + \|\boldsymbol{\pi}_{23}^n - \boldsymbol{\pi}_{23}^{n-1}\|^2\right) + \tau(\nabla p_h^n - \boldsymbol{\pi}_h^{n+\beta-1}, \nabla p_h^n) \qquad (55) \\
-(\delta p_h^n, \nabla\cdot\boldsymbol{u}_h^{n+1}) &= -(\delta p_h^n, \nabla\cdot\hat{\boldsymbol{u}}_h^{n+1}) + \delta t\,(\delta p_h^n, \nabla\cdot(\boldsymbol{\pi}_1^{n+1} - \boldsymbol{\pi}_1^n)) \\
&= \delta t\,(\nabla\delta p_h^n, \nabla\delta p_h^n) + \tau(\nabla p_h^{n+1} - \boldsymbol{\pi}_h^{n+\beta}, \nabla\delta p_h^n) - \delta t\,(\nabla\delta p_h^n, \boldsymbol{\pi}_1^{n+1} - \boldsymbol{\pi}_1^n) \\
&= \delta t\,\|\boldsymbol{\pi}_{23}^n - \boldsymbol{\pi}_{23}^n\|^2 + \tau(\nabla p_h^{n+1} - \boldsymbol{\pi}_h^{n+\beta}, \nabla\delta p_h^n) \qquad (56) \\
-(p_h^{n+1}, \nabla\cdot\hat{\boldsymbol{u}}_h^{n+1}) &= \delta t\,(\nabla\delta p_h^n, \nabla p_h^{n+1}) + \tau(\nabla p_h^{n+1} - \boldsymbol{\pi}_h^{n+\beta}, \nabla p_h^{n+1}) \\
&= \frac{\delta t}{2}\,\left(\|\nabla p_h^{n+1}\|^2 - \|\nabla p_h^n\|^2 + \|\nabla p_h^{n+1} - \nabla p_h^n\|^2\right) \\
&+\tau(\nabla p_h^{n+1} - \boldsymbol{\pi}_h^{n+\beta}, \nabla p_h^{n+1}). \qquad (57)
\end{aligned}$$

The terms multiplied by τ in these expressions can be written as

$$\begin{aligned}
(\nabla p_h^{n+1} - \boldsymbol{\pi}_h^{n+\beta}, \nabla p_h^{n+1}) &= (\boldsymbol{\pi}_3^{n+1}, \nabla p_h^{n+1}) + \bar{\beta}(\boldsymbol{\pi}_h^{n+1} - \boldsymbol{\pi}_h^n, \nabla p_h^{n+1}) \\
&= \|\boldsymbol{\pi}_3^{n+1}\|^2 + \frac{\bar{\beta}}{2}\left(\|\boldsymbol{\pi}_h^{n+1}\|^2 - \|\boldsymbol{\pi}_h^n\|^2 + \|\boldsymbol{\pi}_h^{n+1} - \boldsymbol{\pi}_h^n\|^2\right), \\
(\nabla p_h^{n+1} - \boldsymbol{\pi}_h^{n+\beta}, \nabla\delta p_h^n) &= (\boldsymbol{\pi}_3^{n+1}, \nabla\delta p_h^n) + \bar{\beta}(\boldsymbol{\pi}_h^{n+1} - \boldsymbol{\pi}_h^n, \nabla\delta p_h^n) \\
&= \frac{1}{2}\left(\|\boldsymbol{\pi}_3^{n+1}\|^2 - \|\boldsymbol{\pi}_3^n\|^2 + \|\boldsymbol{\pi}_3^{n+1} - \boldsymbol{\pi}_3^n\|^2\right) + \bar{\beta}\|\boldsymbol{\pi}_h^{n+1} - \boldsymbol{\pi}_h^n\|^2.
\end{aligned}$$

Using these expressions in (55)-(57), the result in (54), and summing for n it is found that

$$\{\boldsymbol{u}_h^n\} \in \ell^\infty(L^2), \quad \{\hat{\boldsymbol{u}}_h^{n+1/2}\} \in \ell^2(H^1),$$
$$\{\delta t\,\nabla p_h^n\} \in \ell^\infty(L^2), \quad \{\sqrt{\delta t}\,\nabla\delta p_h^n\} \in \ell^2(L^2), \quad \{\sqrt{\tau}\,\boldsymbol{\pi}_3^n\} \in \ell^2(L^2).$$

On the other hand, from (53), the inequality $ab \leq (a^2+b^2)/2$ and these stability results it is readily seen that

$$\|\hat{\boldsymbol{u}}_h^{n+1}\|^2 \leq \frac{1}{2}\|\hat{\boldsymbol{u}}_h^{n+1}\|^2 + C\left(\|\boldsymbol{u}_h^n\|^2 + \delta t^{\,2}\|\nabla p_h^n\|^2 + \delta t\,\|\boldsymbol{f}^{n+1/2}\|_{-1}^2\right),$$

from where $\{\hat{\boldsymbol{u}}_h^n\} \in \ell^\infty(L^2)$.

It remains to bound $\boldsymbol{\pi}_1^n$ in $\ell^1(L^2)$. Using the same strategy as for the first order scheme (see (49)), we now have that

$$\delta t\,\sqrt{\tau}\|\boldsymbol{\pi}_1^{n+1}\| \leq \sqrt{\tau}\|\boldsymbol{u}_h^{n+1} - \boldsymbol{u}_h^n\| + \delta t\,\left(N_a\|\hat{\boldsymbol{u}}_h^{n+1/2}\|_1 + N_c\|\hat{\boldsymbol{u}}_h^{n+1/2}\|_1^2\right)$$
$$+\delta t\,\|\boldsymbol{f}^{n+1/2}\|_{-1}.$$

When summing for n, the only term that still has not been shown to be bounded is the first on the right-hand-side. Bounding it will conclude the proof. Since

$$\sum_{n=0}^{N-1}\sqrt{\tau}\|\boldsymbol{u}_h^{n+1}-\boldsymbol{u}_h^n\| \le \sum_{n=0}^{N-1}\sqrt{\tau}\|\boldsymbol{u}_h^{n+1}-\hat{\boldsymbol{u}}_h^{n+1}\| + \sum_{n=0}^{N-1}\sqrt{\tau}\|\hat{\boldsymbol{u}}_h^{n+1}-\boldsymbol{u}_h^n\| \tag{58}$$

and, from (40) and the assumption $\tau \le C\delta t$,

$$\sum_{n=0}^{N-1}\sqrt{\tau}\|\boldsymbol{u}_h^{n+1}-\hat{\boldsymbol{u}}_h^{n+1}\| = \sum_{n=0}^{N-1}\sqrt{\tau}\delta t\,\|\boldsymbol{\pi}_1^{n+1}-\boldsymbol{\pi}_1^n\| \le C\sum_{n=0}^{N-1}\delta t^{\,2}\|\nabla p_h^{n+1}-\nabla p_h^n\|^2 < \infty,$$

it only remains to bound the last term in (58). Taking $\boldsymbol{v}_h = \hat{\boldsymbol{u}}_h^{n+1}-\boldsymbol{u}_h^n$ in (50) and using an inverse estimate similar to (48), it is found that

$$\begin{aligned}
&\frac{1}{\delta t}\|\hat{\boldsymbol{u}}_h^{n+1}-\boldsymbol{u}_h^n\|^2 \le \frac{1}{\sqrt{\tau}}A_n\|\hat{\boldsymbol{u}}_h^{n+1}-\boldsymbol{u}_h^n\| + B_n,\\
&A_n := N_a\|\hat{\boldsymbol{u}}_h^{n+1/2}\|_1 + N_c\|\hat{\boldsymbol{u}}_h^{n+1/2}\|_1^2 + \|\boldsymbol{f}^{n+1/2}\|_{-1},\\
&B_n := (p_h^n, \nabla\cdot\hat{\boldsymbol{u}}_h^{n+1}) - (p_h^n, \nabla\cdot\boldsymbol{u}_h^n).
\end{aligned}$$

Using the fact that if $x^2 \le bx + c$ then $x \le 2b + 2\sqrt{c}$, we obtain

$$\sum_{n=0}^{N-1}\sqrt{\tau}\|\hat{\boldsymbol{u}}_h^{n+1}-\boldsymbol{u}_h^n\| \le C\left(\sum_{n=0}^{N-1}\delta t\,A_n + \sum_{n=0}^{N-1}\sqrt{\delta t}\sqrt{\tau}\sqrt{B_n}\right).$$

The first term on the right-hand-side is bounded, and therefore it only remains to obtain a bound for the second. Since $\tau \le C\delta t$,

$$\sum_{n=0}^{N-1}\sqrt{\delta t}\sqrt{\tau}\sqrt{B_n} \le C\sum_{n=0}^{N-1}\delta t\,B_n.$$

From (55) we have

$$\begin{aligned}
-\sum_{n=0}^{N-1}\delta t\,(p_h^n, \nabla\cdot\boldsymbol{u}_h^n) &\le \frac{1}{2}\sum_{n=0}^{N-1}\delta t^2\,\left(\|\boldsymbol{\pi}_{23}^n\|^2 - \|\boldsymbol{\pi}_{23}^{n-1}\|^2 + \|\boldsymbol{\pi}_{23}^n-\boldsymbol{\pi}_{23}^{n-1}\|^2\right)\\
&+\sum_{n=0}^{N-1}\delta t\,\tau\left[\|\boldsymbol{\pi}_3^n\|^2 + \frac{\bar\beta}{2}\left(\|\boldsymbol{\pi}_h^n\|^2 - \|\boldsymbol{\pi}_h^{n-1}\|^2 + \|\boldsymbol{\pi}_h^n-\boldsymbol{\pi}_h^{n-1}\|^2\right)\right] < \infty,
\end{aligned}$$

and similarly to (55)-(57) we can obtain

$$\begin{aligned}
\sum_{n=0}^{N-1}\delta t\,(p_h^n, \nabla\cdot\hat{\boldsymbol{u}}_h^{n+1}) &= \sum_{n=0}^{N-1}\left[-\delta t^2\,(\nabla\delta p_h^n, \nabla p_h^n) - \delta t\,\tau(\nabla p_h^{n+1}-\boldsymbol{\pi}_h^{n+\beta}, \nabla p_h^n)\right]\\
&= \sum_{n=0}^{N-1}\Bigg[\frac{\delta t^2}{2}\left(\|\nabla p_h^n\|^2 - \|\nabla p_h^{n+1}\|^2 + \|\nabla p_h^n-\nabla p_h^{n+1}\|^2\right)\\
&\qquad -\delta t\,\tau(\boldsymbol{\pi}_3^{n+1}, \boldsymbol{\pi}_3^n) - \delta t\,\tau\bar\beta(\boldsymbol{\pi}_h^{n+1}-\boldsymbol{\pi}_h^n, \boldsymbol{\pi}_h^n)\Bigg]\\
&\le C\sum_{n=0}^{N-1}\delta t^2\,\left(\|\nabla p_h^n-\nabla p_h^{n+1}\|^2 + \|\boldsymbol{\pi}_3^{n+1}\|^2 + \|\boldsymbol{\pi}_3^n\|^2 + \bar\beta\|\boldsymbol{\pi}_h^{n+1}-\boldsymbol{\pi}_h^n\|^2\right) < \infty,
\end{aligned}$$

which completes the proof of stability.

5 Pressure and convection stabilization

The pressure stabilization procedure introduced in the previous section consists of adding the term

$$\tau(\nabla p_h^{n+1} - \boldsymbol{\pi}_h^n, \nabla q_h)$$

to the variational equations of the Galerkin method (either to the monolithic or to the fractional step time discretization). We have considered directly the case $\beta = 0$, which is more appealing from the computational point of view and has the same stability properties as the case $\beta = 1$. This stabilizing term can be thought of as a least-squares form of the component of the pressure gradient orthogonal to the finite element space, $\boldsymbol{\pi}_3^{n+1} = \nabla p_h^{n+1} - \boldsymbol{\pi}_h^{n+1}$. If this allows to stabilize the pressure, the idea that naturally arises is to use the same strategy to stabilize convection when the convective term dominates the viscous one. This idea is developed in [23]. Here we describe only the final outcome, which consists of adding

$$\tau(\hat{\boldsymbol{u}}_h^{n+\theta} \cdot \nabla \hat{\boldsymbol{u}}_h^{n+\theta} + \nabla p_h^{n+1} - \boldsymbol{\pi}_h^n \ , \ \hat{\boldsymbol{u}}_h^{n+\theta} \cdot \nabla \boldsymbol{v}_h + \nabla q_h)$$

to the variational equations of the Galerkin method. The contribution to the momentum equation is obtained when the pressure test function is $q_h = 0$, whereas the contribution to the continuity equation is found when $\boldsymbol{v}_h = \boldsymbol{0}$. The final result is that the equations to be solved when fractional step methods are used are

$$\begin{aligned}
&\frac{1}{\delta t}(\hat{\boldsymbol{u}}_h^{n+1} - \boldsymbol{u}_h^n, \boldsymbol{v}_h) + c(\hat{\boldsymbol{u}}_h^{n+\theta}, \hat{\boldsymbol{u}}_h^{n+\theta}, \boldsymbol{v}_h) + a(\hat{\boldsymbol{u}}_h^{n+\theta}, \boldsymbol{v}_h) - \gamma b(p_h^n, \boldsymbol{v}_h) \\
&\qquad + \tau(\hat{\boldsymbol{u}}_h^{n+\theta} \cdot \nabla \hat{\boldsymbol{u}}_h^{n+\theta} + \nabla p_h^n - \boldsymbol{\pi}_h^n \ , \ \hat{\boldsymbol{u}}_h^{n+\theta} \cdot \nabla \boldsymbol{v}_h) = \langle \boldsymbol{f}^{n+\theta}, \boldsymbol{v}_h \rangle \quad \forall \boldsymbol{v}_h \in \boldsymbol{V}_h, \\
&-\delta t\,(\nabla(p_h^{n+1} - \gamma p_h^n), \nabla q_h) - \tau(\hat{\boldsymbol{u}}_h^{n+\theta} \cdot \nabla \hat{\boldsymbol{u}}_h^{n+\theta} + \nabla p_h^{n+1} - \boldsymbol{\pi}_h^n, \nabla q_h) \\
&\qquad = (q_h, \nabla \cdot \hat{\boldsymbol{u}}_h^{n+1}) \quad \forall q_h \in Q_h, \\
&\frac{1}{\delta t}(\boldsymbol{u}_h^{n+1} - \hat{\boldsymbol{u}}_h^{n+1}, \boldsymbol{v}_h) - b(p_h^{n+1} - \gamma p_h^n, \boldsymbol{v}_h) = 0 \quad \forall \boldsymbol{v}_h \in \boldsymbol{V}_h, \\
&(\boldsymbol{\pi}_h^{n+1}, \boldsymbol{\eta}_h) = (\hat{\boldsymbol{u}}_h^{n+\theta} \cdot \nabla \hat{\boldsymbol{u}}_h^{n+\theta} + \nabla p_h^{n+1}, \boldsymbol{\eta}_h) \quad \forall \boldsymbol{\eta}_h \in \tilde{\boldsymbol{V}}_h,
\end{aligned}$$

which replace (36)-(39). It has to be observed that the pressure in the first equation is treated explicitly, in order to keep the uncoupling of the velocity and pressure calculations. Observe also that now $\boldsymbol{\pi}_h$ has the meaning of being the projection of $\hat{\boldsymbol{u}}_h \cdot \nabla \hat{\boldsymbol{u}}_h + \nabla p_h$ onto the finite element space.

Let us finally remark the possibility of treating explicitly the projection $\boldsymbol{\pi}_h$ greatly simplifies the numerical implementation of this stabilization technique. Apart from the evaluation of the several additional terms in the equations for the velocity and the pressure, only an L^2 projection needs to be performed at the end of each time step. This is computationally very inexpensive, especially if the Gramm matrix $\tilde{\mathsf{M}}$ involved in the process is approximated by the diagonal one obtained from a standard lumping technique.

6 Numerical results

In this section we present the result of two simple 2D numerical experiments to illustrate the practical impact of the theoretical findings. The objective of the first is to show the dependence of the pressure stability on the time step, whereas the second is mainly intended to check the accuracy, a point that has been mentioned but not analyzed.

6.1 Cavity flow problem

This example is the classical cavity flow problem. The Navier-Stokes equations are solved in the unit square with zero velocities everywhere on the boundary except on the top, where a tangent unit velocity is prescribed. The viscosity has been taken as $\nu = 0.01$, which yields a Reynolds number of 100. A mesh of 20×20 four-noded bilinear elements has been employed. The flow equations have been advanced in time until the steady-state has been reached. The critical time step for the explicit scheme has been estimated to be

$$\delta t_{\,\mathrm{crit}} = \left(\frac{4\nu}{h^2} + \frac{2U}{h} \right)^{-1} , \tag{59}$$

where $h = 0.05$ is the element size and $U = 1$ the characteristic velocity. This yields $\delta t_{\,\mathrm{crit}} = 1/56$.

Pressure contours using the original first order scheme are shown in Fig. 1. It is clearly observed there that for $\delta t = 0.1\,\delta t_{\,\mathrm{crit}}$ some oscillations appear, whereas for $\delta t = \delta t_{\,\mathrm{crit}}$ the solution is acceptable. Likewise, when δt is large (1 in this case), the solution is definitely overdiffusive. This shows the dependence of the pressure stability on the time step size.

The same cases have been computed with the second order scheme. From Fig. 2 it is seen that only for very large values of δt the weak stability inherent to the scheme is activated. Contrary to the previous case, for $\delta t = 0.1\,\delta t_{\,\mathrm{crit}}$ and $\delta t = \delta t_{\,\mathrm{crit}}$ the pressure solution is completely oscillatory.

The final set of results for this problem shown in Fig. 3 corresponds to the stabilized formulation using the second order scheme. The stability parameter τ has been computed as the critical time step given by (59) but for each element, taking U as the mean element velocity. The pressure solution is correct for all the values of δt.

Even though the implicit schemes we have considered allow us to use time steps as large as desired, it is known that in practice the steady-state is reached faster (both in real time and in CPU time) using δt close to $\delta t_{\,\mathrm{crit}}$. We have also used this example to demonstrate this. Converge to the steady-state for the different formulations employed is shown in Fig. 4, where the residual is measured as $|\mathsf{U}^n - \mathsf{U}^{n-1}|/|\mathsf{U}^1 - \mathsf{U}^0|$ (here $|\cdot|$ is the standard Euclidean norm of an array). From Fig. 5 it is seen that this dependence on δt is similar for all the schemes.

6.2 A test with analytical solution

We have referred to the two formulations analyzed throughout the paper as the *first* order projection method and a *second* order scheme. In this example we test the accuracy of these formulations. Since we have seen that the second order one is unstable, we have combined it with the pressure stabilization technique, with the parameter τ computed as in the previous test.

In this example we solve again the Navier-Stokes equations in the unit square with homogeneous velocity conditions and taking the force vector so as to have as exact solution

$$u_1(x_1,x_2,t) = f(x_1)f'(x_2)g(t), \quad u_1(x_1,x_2,t) = -f'(x_1)f(x_2)g(t), \tag{60}$$
$$f(x) = 100x^2(1-x)^2, \quad g(t) = \cos(\pi t)\exp(-t),$$

with two solutions for the pressure, namely, $p = 0$ and $p = 100x^2$. The time interval of analysis is $[0,1]$ and the viscosity $\nu = 0.1$. A mesh of 40×40 bilinear elements has been employed to discretize the computational domain. The velocity solution at $t = 1$ is shown in Fig. 6.

Convergence of the time approximation for the case $p = 0$ and measured at $t = 1$ is plotted in Fig. 7, where 'total' refers to the scheme with $\gamma = 0$ in (15)-(17) and 'incremental' to the case $\gamma = 1$. The error has been computed as $|\mathsf{U}_{t=1} - \mathsf{U}_{\text{exact}}|/|\mathsf{U}_{\text{exact}}|$, where $\mathsf{U}_{t=1}$ is the numerical solution at $t = 1$ and $\mathsf{U}_{\text{exact}}$ the array of nodal values of the exact velocity at $t = 1$. Since the exact pressure is $p = 0$, the value of γ does not affect the accuracy in this example. From Fig. 7 it is seen that $\theta = 1$ gives a first order approximation and $\theta = 1/2$ a second order one. The evolution of the first velocity component u_1 at a point is depicted in Fig. 8 and Fig. 9 for the first and second order schemes, respectively.

The evolution to the steady-state when $g(t)$ is replaced by 1 in (60) is shown in Fig. 10. As in the previous example, it is seen that large values of δt may yield slower rates of convergence. Finally, Fig. 11 shows the error at the steady-state as a function of δt when $p = 100x^2$, measuring the well known property that for the first order scheme the solution depends largely on δt.

7 Summary of main results and conclusions

The main objective of this paper has been to clarify the role of the pressure Poisson equation in the pressure stability of fractional step methods for incompressible flows, in our case using the finite element method for the space discretization. The basic stability results for the two schemes analyzed are:

First order:	$\{\sqrt{\delta t}\,\nabla p_h^n\} \in \ell^2(L^2)$,		$\{\sqrt{\tau}\nabla p_h^n\} \in \ell^1(L^2)$
Second order:	$\{\delta t\,\nabla p_h^n\} \in \ell^\infty(L^2)$,	$\{\sqrt{\delta t}\,\nabla \delta p_h^n\} \in \ell^2(L^2)$,	$\{\sqrt{\tau}\,\nabla p_h^n\} \in \ell^1(L^2)$

Inspecting these results, the main conclusions that can be drawn are:

- For the original ($\tau = 0$) first order scheme, pressure is stable, but the parameter that controls the amount of stability is the time step size, and therefore:
  - If δt is very small, pressure oscillations may appear.
  - If δt is large, the method may be overdiffusive. This limits the applicability of implicit schemes, since appropriate values of δt adequate for stability turn out to be close to the critical time step of explicit schemes ($\theta = 0$).
- The original ($\tau = 0$) second order method has a very poor pressure stability, although it may be active if δt is very large. At the steady-state, only that $\delta t \, \|\nabla p_h\| < \infty$ can be ensured, whereas the optimum would be to have control on $\sqrt{\delta t} \, \|\nabla p_h\|$.
- Pressure stability in stabilized schemes depends on an algorithmic parameter τ, which may be chosen independent of δt (except for the condition $\tau \leq C\delta t$ needed for the second order scheme). Both for the first and for the second order methods, this stabilization allows us to free the link stability–δt.

A very important fact from the computational point of view is that the pressure gradient projection for stabilized schemes *may be treated explicitly* (which corresponds to taking $\beta = 0$ in (37)). It has been shown that this does not upset stability. Finally, let us mention that convection dominated flows can be stabilized by considering a natural extension of the pressure stabilization technique which has been described in Section 5.

References

[1] A.J. Chorin. A numerical method for solving incompressible viscous problems. *Journal of Computational Physics*, 2:12–26, 1967.

[2] R. Temam. Sur l'approximation de la solution des équations de Navier–Stokes par la méthode des pas fractionaires (I). *Archives for Rational Mechanics and Analysis*, 32:135–153, 1969.

[3] R. Natarajan. A numerical method for incompressible viscous flow simulation. *Journal of Computational Physics*, 100:384–395, 1992.

[4] J. Shen. Hopf bifurcation of the unsteady regularized driven cavity-flow. *Journal of Computational Physics*, 95:228–245, 1991.

[5] S. Turek. A comparative study of time-stepping techniques for the incompressible Navier-Stokes equations: from fully implicit nonlinear schemes to semi-implicit projection methods. *International Journal for Numerical Methods in Fluids*, 22:987–1011, 1996.

[6] R. Temam. Remark on the pressure boundary condition for the projection method. *Theoretical Computational Fluid Dynamics*, 3:181–184, 1991.

[7] P.M. Gresho. On the theory of semi-implicit projection methods for viscous incompressible flow and its implementation via a finite element method that also introduces a nearly consistent mass matrix. Part I: Theory. *International Journal for Numerical Methods in Fluids*, 11:587–620, 1990.

[8] J.B. Perot. An analysis of the fractional step method. *Journal of Computational Physics*, 108:51–58, 1993.

[9] A. Quarteroni, F. Saleri, and A. Veneziani. Factorization methods for the numerical approximation of Navier-Stokes equations. *Computer Methods in Applied Mechanics and Engineering*, to appear.

[10] J. Shen. On error estimates of projection methods for Navier-Stokes equations: first order squemes. *SIAM Journal on Numerical Analysis*, 29:57–77, 1992.

[11] J. Shen. On error estimates for some higher order projection and penalty-projection methods for Navier-Stokes equations. *Numerische Mathematik*, 62:49–73, 1992.

[12] J.L. Guermond and L. Quartapelle. On the approximation of the unsteady Navier-Stokes equations by finite element projection methods. *Numerische Mathematik*, 80:207–238, 1998.

[13] J. C. Strikwerda and Y. S. Lee. The accuracy of the fractional step method. *SIAM Journal on Numerical Analysis*, 37:37–47, 1999.

[14] J.L. Guermond and L. Quartapelle. On stability and convergence of projection methods based on pressure Poisson equation. *International Journal for Numerical Methods in Fluids*, 26:1039–1053, 1998.

[15] J.B. Bell, P. Colella, and H.M. Glaz. A second-order projection method for the incompressible Navier-Stokes equations. *Journal of Computational Physics*, 85:257–283, 1989.

[16] G.E. Karniadakis, M. Israeli, and S.E. Orzag. High order splitting methods for the incompressible Navier-Stokes equations. *Journal of Computational Physics*, 59:414–443, 1991.

[17] J. Kim and P. Moin. Application of the fractional step method to incompressible Navier-Stokes equations. *Journal of Computational Physics*, 59:308–323, 1985.

[18] J. van Kan. A second–order accurate pressure correction scheme for viscous incompressible flow. *SIAM Journal of Sci. Stat. Comp.*, 7:870–891, 1986.

[19] R. Codina. Numerical solution of the incompressible Navier-Stokes equations with Coriolis forces based on the discretization of the total time derivative. *Journal of Computational Physics*, 148:467–496, 1999.

[20] R. Codina and J. Blasco. A finite element formulation for the Stokes problem allowing equal velocity-pressure interpolation. *Computer Methods in Applied Mechanics and Engineering*, 143:373–391, 1997.

[21] R. Codina and J. Blasco. Analysis of a pressure-stabilized finite element approximation of the stationary Navier-Stokes equations. *Numerische Mathematik*, to appear.

[22] R. Codina and J. Blasco. Stabilized finite element method for the transient Navier-Stokes equations based on a pressure gradient projection. *Computer Methods in Applied Mechanics and Engineering*, 182:287–310, 2000.

[23] R. Codina. Stabilization of incompressibility and convection through orthogonal subscales in finite element methods. *Computer Methods in Applied Mechanics and Engineering*, to appear.

[24] J.G. Heywood and R. Rannacher. Finite element approximation of the nonstationary Navier-Stokes problem. IV: Error analysis for second-order time discretization. *SIAM Journal on Numerical Analysis*, 27:353–384, 1990.

[25] F. Brezzi and M. Fortin. *Mixed and hybrid finite element methods.* Springer Verlag, 1991.

[26] G.E. Schneider, G.D. Raithby, and M.M. Yovanovich. Finite element analysis of incompressible fluid flow incorporating equal order pressure and velocity interpolation. In *Numerical Methods in Laminar and Turbulent Flow* (C. Taylor, K. Morgan, C.A. Brebbia eds). Pentech Press, Plymouth, 1978.

[27] M. Kawahara and K. Ohmiya. Finite element analysis of density flow using the velocity correction method. *International Journal for Numerical Methods in Fluids*, 5:981–993, 1985.

[28] O.C. Zienkiewicz and R. Codina. A general algorithm for compressible and incompressible flow—Part I. The split, characteristic-based scheme. *International Journal for Numerical Methods in Fluids*, 20:869–885, 1995.

[29] H.G. Choi, H. Choi, and J.Y. Yoo. A fractional four-step finite element formulation of the unsteady incompressible Navier-Stokes equations using supg and linear equal-order

element methods. *Computer Methods in Applied Mechanics and Engineering*, 143:333–348, 1997.

[30] T.J.R. Hughes, L.P. Franca, and M. Balestra. A new finite element formulation for computational fluid dynamics: V. Circumventing the Babuška-Brezzi condition: a stable Petrov-Galerkin formulation for the Stokes problem accommodating equal-order interpolations. *Computer Methods in Applied Mechanics and Engineering*, 59:85–99, 1986.

[31] L. Franca and R. Stenberg. Error analysis of some Galerkin least-squares methods for the elasticity equations. *SIAM Journal on Numerical Analysis*, 28:1680–1697, 1991.

[32] L.P. Franca and S.L. Frey. Stabilized finite element methods: II. The incompressible Navier-Stokes equations. *Computer Methods in Applied Mechanics and Engineering*, 99:209–233, 1992.

[33] F. Brezzi and J. Douglas. Stabilized mixed methods for the Stokes problem. *Numerische Mathematik*, 53:225–235, 1988.

[34] R. Rannacher. *On Chorin's projection method for incompressible Navier-Stokes equations,* Lecture Notes in Mathematics, volume 1530, pages 167–183. Springer, Berlin, 1992.

[35] J.L. Guermond and L. Quartapelle. Calculation of incompressible flows by an unconditionally stable FEM algorithm. *Journal of Computational Physics*, 132:12–33, 1997.

[36] R. Codina, M. Vázquez, and O.C. Zienkiewicz. A general algorithm for compressible and incompressible flow—Part III. The semi-implicit form. *International Journal for Numerical Methods in Fluids*, 27:13–32, 1998.

[37] S.C. Brenner and L.R. Scott. *The mathematical theory of finite element methods.* Springer–Verlag, 1994.

List of Figures

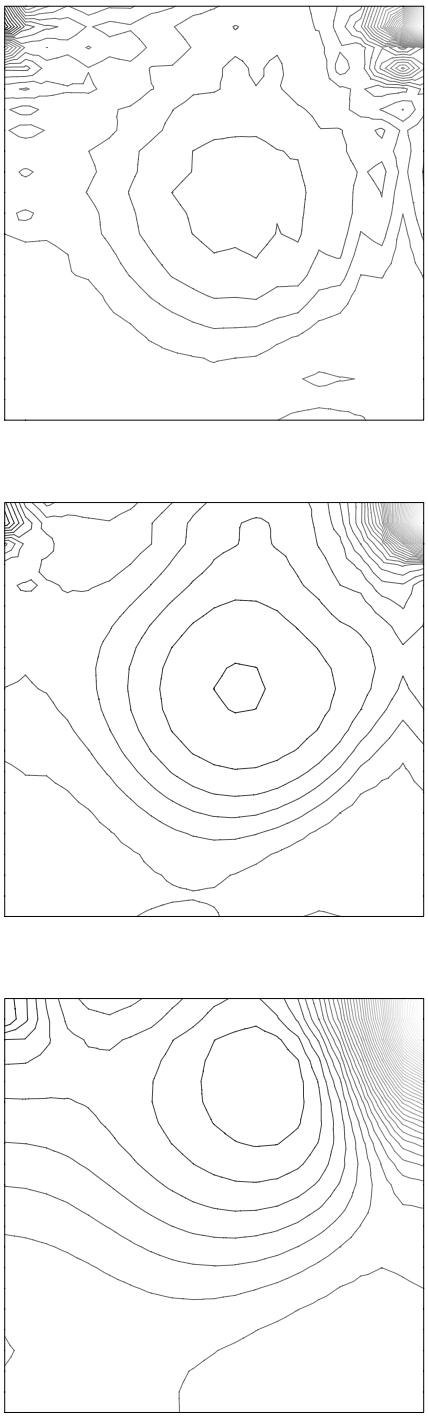

Figure 1: Pressure contours for the cavity flow problem using the first order scheme. From the top to the bottom: $\delta t = 0.1\,\delta t_{\text{crit}}$, $\delta t = \delta t_{\text{crit}}$ and $\delta t = 1.0$.

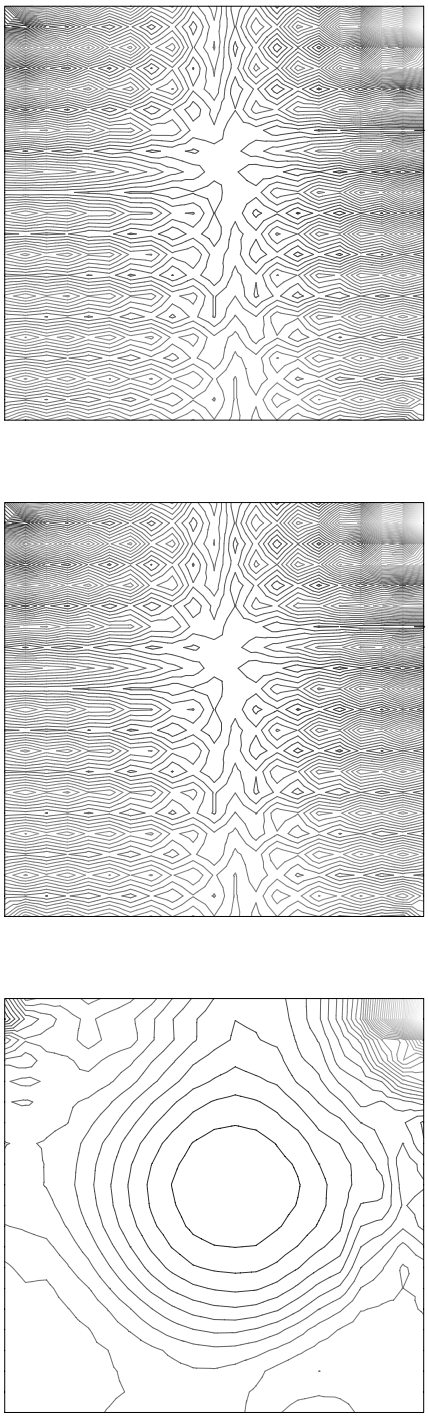

Figure 2: Pressure contours for the cavity flow problem using the second order scheme. From the top to the bottom: $\delta t = 0.1\,\delta t_{\text{crit}}$, $\delta t = \delta t_{\text{crit}}$ and $\delta t = 1.0$.

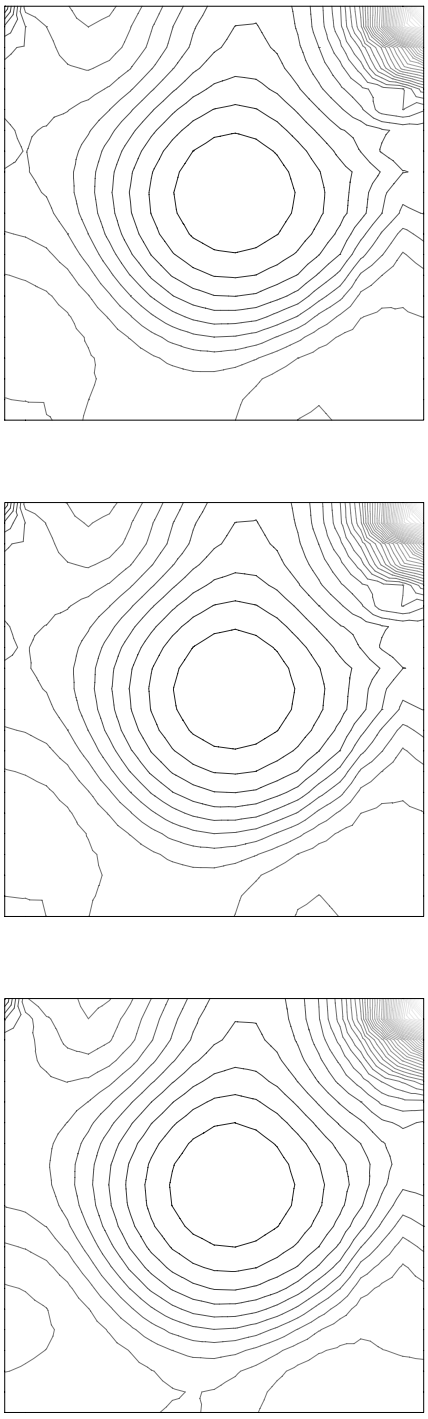

Figure 3: Pressure contours for the cavity flow problem using the second order scheme with stabilization. From the top to the bottom: $\delta t = 0.1\,\delta t_{\text{crit}}$, $\delta t = \delta t_{\text{crit}}$ and $\delta t = 1.0$.

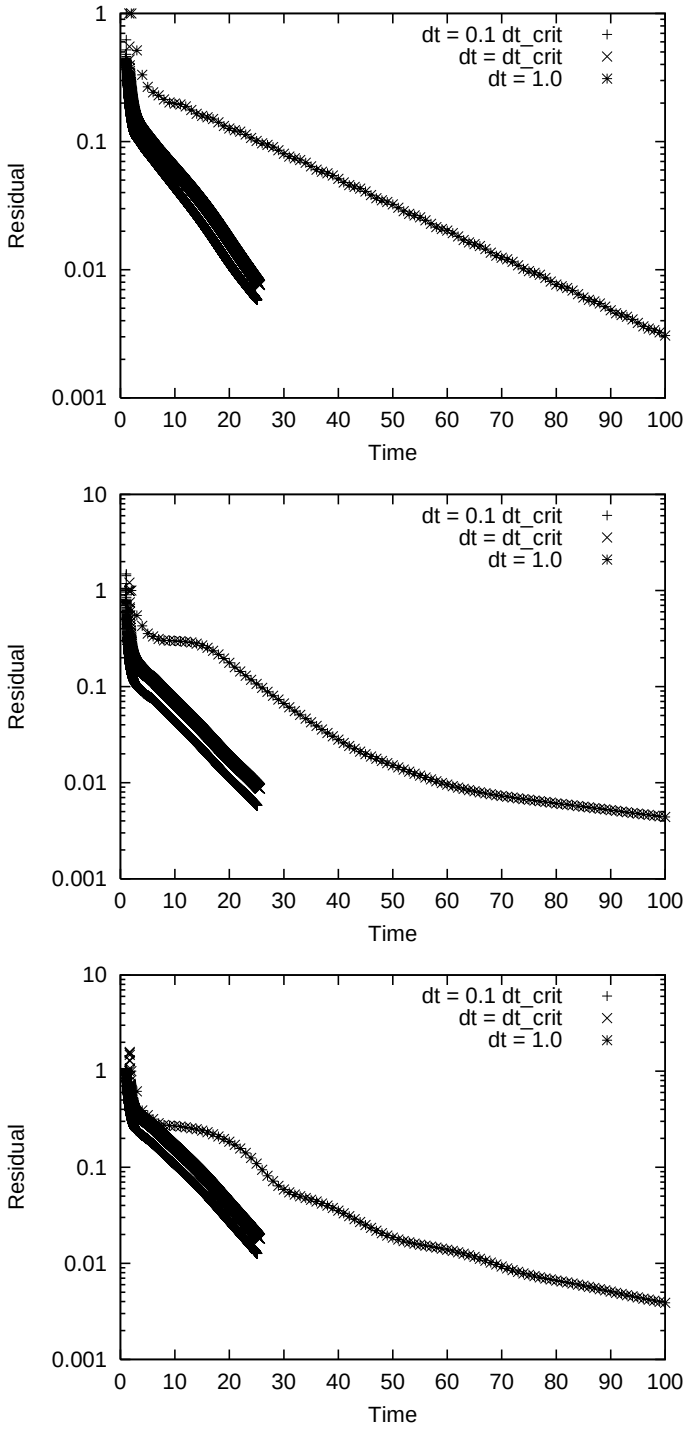

Figure 4: Velocity convergence towards the steady state for the cavity flow problem. From the top to the bottom: first order scheme, second order scheme and second order scheme with stabilization.

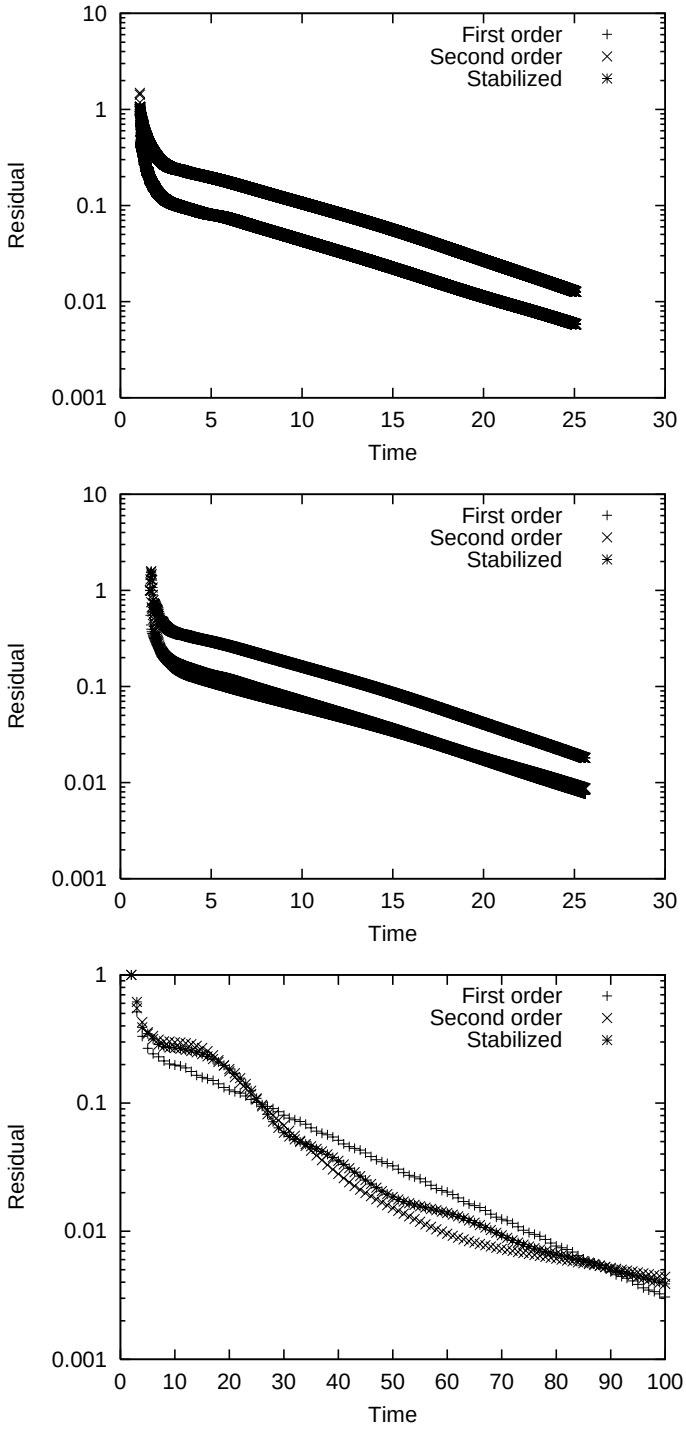

Figure 5: Velocity convergence towards the steady state for the cavity flow problem. From the top to the bottom: $\delta t = 0.1\,\delta t_{\text{crit}}$, $\delta t = \delta t_{\text{crit}}$ and $\delta t = 1.0$.

Figure 6: Velocity vectors for the test with analytical solution.

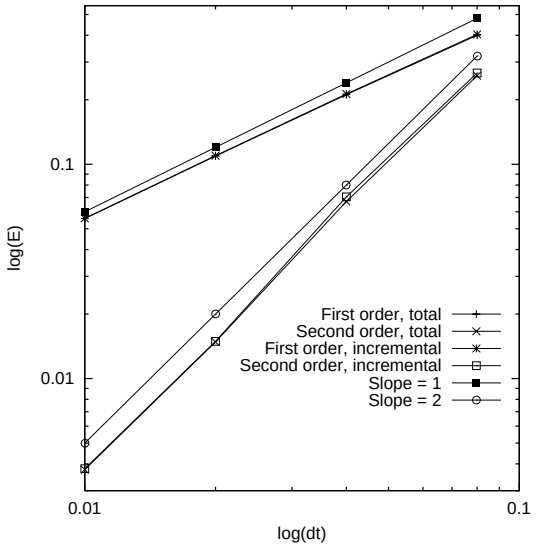

Figure 7: Convergence for the test with analytical solution. Case $p = 0$.

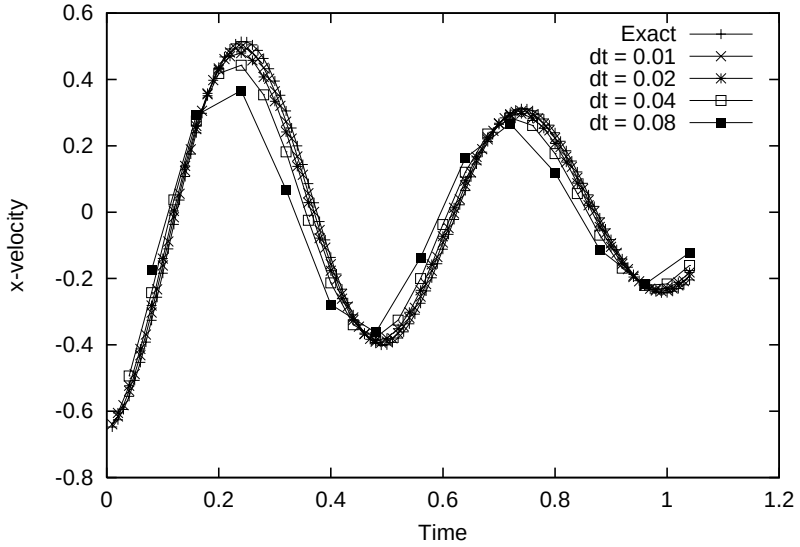

Figure 8: Evolution of the x-velocity at $(0.75, 0.75)$ using the a first order scheme. Case $p = 0$.

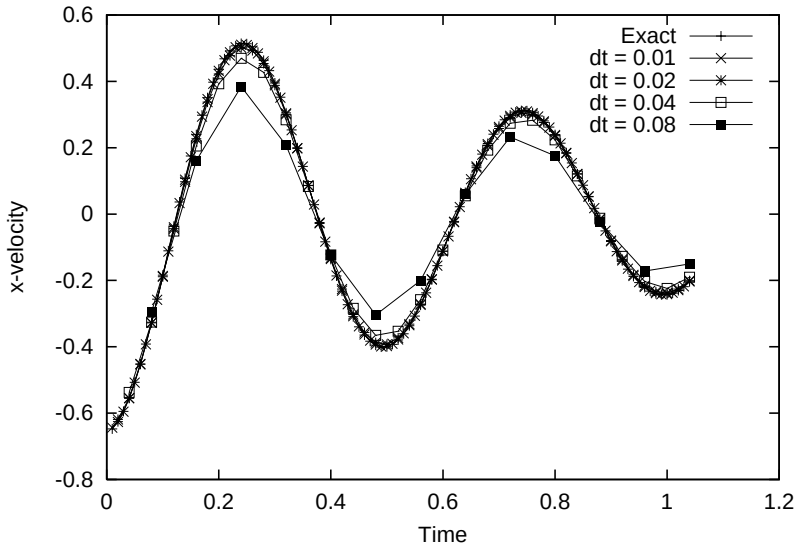

Figure 9: Evolution of the x-velocity at $(0.75, 0.75)$ using the a second order scheme. Case $p = 0$.

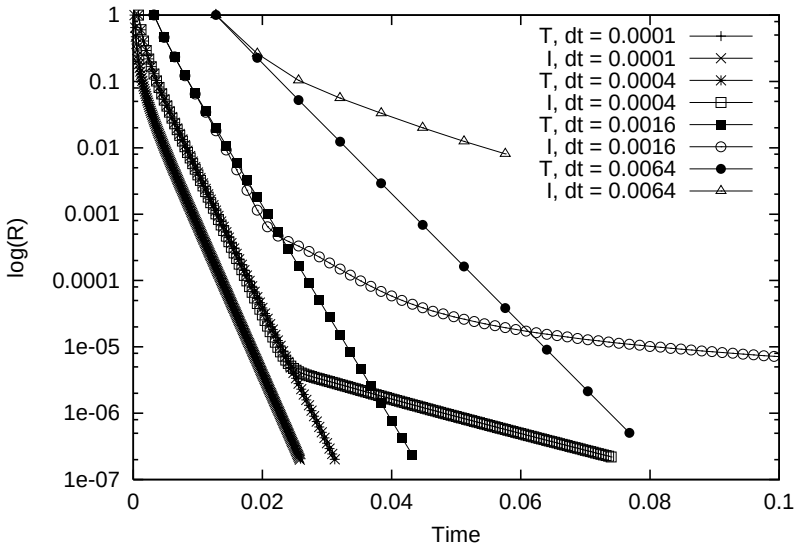

Figure 10: Convergence to the steady-state for the test with analytical solution (T: total, I: incremental). Case $p = 100x^2$.

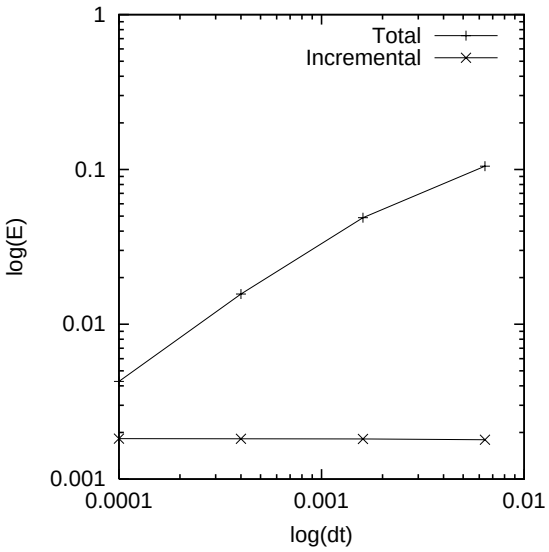

Figure 11: Error at the steady-state as a function of the time step for the test with analytical solution. Case $p = 100\,x^2$.